



HAL
open science

Discovery of a Locally and Orally Active CXCL12 Neutraligand (LIT-927) with Anti-inflammatory Effect in a Murine Model of Allergic Airway Hypereosinophilia

Pierre Regenass, Dayana Abboud, François Daubeuf, Christine Lehalle, Patrick Gizzi, Stéphanie Riché, Muriel Hachet-Haas, François Rohmer, Vincent Gasparik, Damien Boeglin, et al.

► To cite this version:

Pierre Regenass, Dayana Abboud, François Daubeuf, Christine Lehalle, Patrick Gizzi, et al.. Discovery of a Locally and Orally Active CXCL12 Neutraligand (LIT-927) with Anti-inflammatory Effect in a Murine Model of Allergic Airway Hypereosinophilia. *Journal of Medicinal Chemistry*, 2018, 61 (17), pp.7671-7686. 10.1021/acs.jmedchem.8b00657 . hal-03563473

HAL Id: hal-03563473

<https://hal.science/hal-03563473>

Submitted on 9 Feb 2022

HAL is a multi-disciplinary open access archive for the deposit and dissemination of scientific research documents, whether they are published or not. The documents may come from teaching and research institutions in France or abroad, or from public or private research centers.

L'archive ouverte pluridisciplinaire **HAL**, est destinée au dépôt et à la diffusion de documents scientifiques de niveau recherche, publiés ou non, émanant des établissements d'enseignement et de recherche français ou étrangers, des laboratoires publics ou privés.

1
2
3 **Discovery of a Locally and Orally Active CXCL12 Neutraligand (LIT-927) with Anti-**
4 **inflammatory Effect in a Murine Model of Allergic Airway Hypereosinophilia**
5
6
7
8
9

10 Pierre Regenass^{1,4}, Dayana Abboud^{2,4}, François Daubeuf^{1,4}, Christine Lehalle^{1,4}, Patrick Gizzi^{3,4},
11 Stéphanie Riché^{1,4}, Muriel Hachet-Haas^{2,4}, François Rohmer^{1,4}, Vincent Gasparik^{1,4}, Damien Boeglin^{1,4},
12 Jacques Haiech^{1,4}, Tim Knehans^{1,4}, Didier Rognan^{1,4}, Denis Heissler^{1,4}, Claire Marsol^{1,4}, Pascal Villa^{3,4},
13 Jean-Luc Galzi^{2,4}, Marcel Hibert^{1,4}, Nelly Frossard^{1,4*}, Dominique Bonnet^{1,4*}
14
15
16
17
18
19
20
21

22 ¹ Laboratoire d'Innovation Thérapeutique, Faculté de Pharmacie, UMR7200 CNRS/Université de
23 Strasbourg, 74 route du Rhin, 67401 Illkirch, France.
24

25 ² Biotechnologie et Signalisation Cellulaire, Ecole Supérieure de Biotechnologie de Strasbourg, UMR
26 7242 CNRS/Université de Strasbourg, Bld Sébastien Brant, 67412 Illkirch, France.
27
28

29 ³ Plate-forme de chimie biologique intégrative de Strasbourg, UMS 3286 CNRS/Université de
30 Strasbourg, 67412 Illkirch, France.
31
32
33

34 ⁴ Labex MEDALIS, Université de Strasbourg, 67000 Strasbourg, France.
35
36
37
38
39
40
41
42
43
44
45
46
47
48
49
50
51
52
53
54
55
56
57
58
59
60

ABSTRACT

We previously reported Chalcone-4 (**1**) that binds the chemokine CXCL12, not its cognate receptors CXCR4 or CXCR7, and neutralizes its biological activity. However, this neutraligand suffers from limitations such as poor chemical stability, solubility and oral activity. Herein, we report on the discovery of pyrimidinone **57** (LIT-927), a novel neutraligand of CXCL12 which displays a higher solubility than **1** and is no longer Michael acceptor. While both **1** and **57** reduce eosinophil recruitment in a murine model of allergic airway hypereosinophilia, **57** is the only one to display inhibitory activity following oral administration. Thereby, we here describe **57** as the first orally active CXCL12 neutraligand with anti-inflammatory properties. Combined with a high binding selectivity for CXCL12 over other chemokines, **57** represents a powerful pharmacological tool to investigate CXCL12 physiology *in vivo*, and to explore the activity of chemokine neutralization in inflammatory and related diseases.

INTRODUCTION

Chemokines are small proteins with critical roles in the development and function of various tissues in vertebrates.^{1,2,3} As a rather general rule, chemokines and their G protein-coupled receptors display redundancy and binding promiscuity, i.e. one chemokine may bind to different receptors,^{4,5} whereas chemokine receptors may be activated by various chemokines. A few chemokines play a pivotal and non-redundant homeostatic role, as is the case for CXCL12. In the adult, they regulate the directional migration of leukocytes under normal and pathological conditions.⁶ They are associated with an extraordinary high number of diseases, including chronic inflammation,⁶ autoimmune diseases (lupus erythematosus),⁷ cancer^{8,9} atherosclerosis^{10,11} or AIDS ;¹² their receptors have been considered as druggable targets.¹³ Indeed, classical drug design strategies aim at discovering chemokine receptor ligands, mainly antagonists, in order to regulate the associated functions.^{14,15} Yet, many antagonists have disappointingly failed in clinical trials, which may be related either to chemokine receptor redundancy, or to the difficulty of designing specific chemokine receptor antagonists.^{16,17} We have recently opened a novel avenue for drug development in reporting a small molecule, “Chalcone-4” (**1**), that displays an original mechanism of action as it binds to the chemokine CXCL12, not to its two cognate receptors CXCR4 and CXCR7, and neutralizes its biological activity.¹⁸ Chalcone-4 and related molecules have been termed “neutraligands” by analogy with neutralizing antibodies, and proved to have therapeutic potential. Indeed, **1** inhibits binding of CXCL12 to CXCR4 and CXCR7, reduces intracellular calcium responses, blocks chemotaxis of human peripheral blood CD4⁺ lymphocytes, and prevents CXCR4 internalization in response to CXCL12.¹⁸ This chemical compound is active *in vivo* in a mouse model of allergic airway eosinophilic inflammation, where it inhibits eosinophil infiltration in response to the allergen. It is also active in other disease models involving the CXCL12/CXCR4 axis such as the WHIM syndrome or carcinogenesis.^{19,20} As the poor solubility of **1** prevented its local administration in the

1
2
3 airways, we have previously successfully developed simple analogues of **1** acting as prodrugs to
4
5 improve solubility, and showed that a significant local bronchial activity was reached at low dose.²¹ We
6
7 have also developed an antedrug active when administered locally, and inactivated when passing
8
9 systemically, thereby preventing distant adverse events, and thus optimizing the specificity of action.²²
10
11 Therefore, neutralizing CXCL12 by small compounds has proven to be a promising strategy to treat
12
13 inflammatory diseases, in particular asthma. However, all these neutraligands encompass a chalcone
14
15 chemotype and display major limitations including Michael acceptor character and poor oral activity.
16
17 Very few other small organic compounds able to bind CXCL12 have been reported to date. Recently, *in*
18
19 *silico* screening led to the identification of ZINC 310454,²³ obtained following a fragment-based
20
21 structure-activity relationship (SAR) analysis,²⁴ with some activity on cell migration *in vitro* at μM
22
23 concentrations. Other small molecule ligands have been identified for different binding sites on
24
25 CXCL12, but neither *in vitro* nor *in vivo* activity have been reported yet.²⁵ Another example is the
26
27 aptamer NOX-A12 that shows anti CXCL12 activity *in vitro* and *in vivo*, but is not orally bioavailable.²⁶
28
29 Here, we describe a systematic SAR study around **1** and the discovery of the first selective and orally
30
31 active CXCL12 neutraligand **57** (LIT-927) derived from a pyrimidinone scaffold in an allergic airway
32
33 eosinophilic inflammation in the mouse.
34
35
36
37
38
39
40
41
42
43
44
45
46
47
48
49
50
51
52
53
54
55
56
57
58
59
60

RESULTS AND DISCUSSION

The physiological and pathophysiological importance of CXCL12 and CXCR4 has prompted us to launch drug discovery programs for various diseases. Chalcone-4 (**1**), previously identified following a high throughput screening approach, binds to CXCL12, thereby preventing interaction with CXCR4.¹⁸ However, **1** displays also some major drawbacks for drug development: 1) its solubility in aqueous media is low (9 μ M in PBS buffer); 2) the presence of the α,β -unsaturated carbonyl group (often referred to as Michael acceptors) allows 1,4-additions with thiols;²⁷ 3) it is not active *in vivo* in murine models of allergic airway hypereosinophilia by the oral route.

To overcome these limitations, **1** was selected as the starting point for further structural optimization. The modular nature of this compound made it particularly well suited for utilization of array synthesis to efficiently explore the SAR of the chemotype. Optimization efforts went along four directions: i) exploration of the substitution on ring A, ii) on ring B, iii) modification of the central core (CC) of **1**, and iv) design of rigid isosteres (Figure 1).

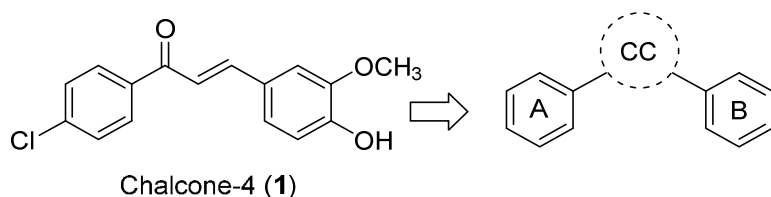
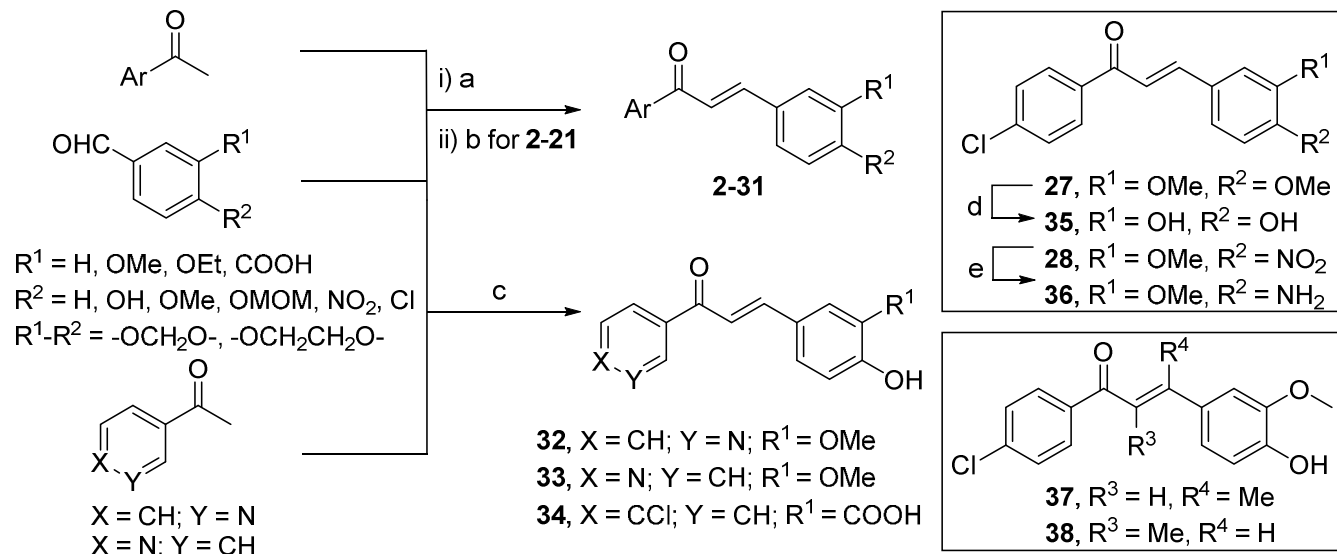


Figure 1. SAR strategy around Chalcone-4 (**1**).

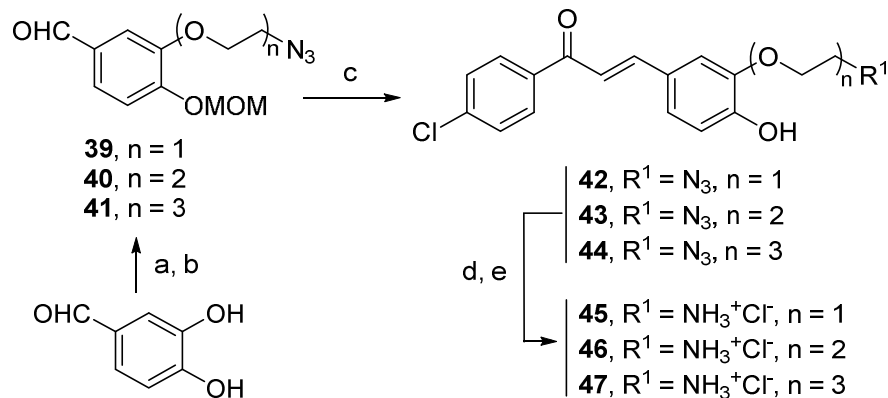
1
2
3 **Synthesis.** Chalcones **2-31** were prepared from an acetophenone and a benzaldehyde by a Claisen-
4 Schmidt reaction using barium hydroxide hydrate as a base.²⁸ When necessary, methoxymethyl (MOM)
5 deprotection was carried out with concentrated hydrochloric acid in THF (Scheme 1). In some cases, the
6 condensation was advantageously performed under acidic conditions by bubbling hydrogen chloride
7 through a dichloromethane solution of the reagents (**32** and **33**) or using a mixture of aqueous hydrogen
8 chloride and sulfuric acid (**34**). Interestingly, compound **1** was best synthesized by carefully adding
9 thionyl chloride to an ethanolic solution of the two carbonyl partners, thus generating hydrogen chloride
10 *in situ*. In some cases, additional steps were required. Thus, amino derivative **36** was prepared by
11 reduction of the corresponding nitro precursor **28** in the presence of iron in acidic ethanol, whereas **35**
12 was obtained by demethylation of the methoxy substituents with boron tribromide in dichloromethane.
13 Chalcone **37** was prepared from 1-(4-chlorophenyl)but-2-yn-1-one and (4-bromo-2-methoxyphenoxy)
14 (tert-butyl)dimethylsilane using *n*-butyllithium and copper(I) bromide, followed by deprotection of
15 TBDMS with sodium hydroxide. Chalcone **38** was obtained by treatment of the corresponding carbonyl
16 compounds with pyridinium acetate/piperidine.
17
18
19
20
21
22
23
24
25
26
27
28
29
30
31
32
33
34
35
36
37
38
39
40
41
42
43
44
45
46
47
48
49
50
51
52
53
54
55
56
57
58
59
60

Scheme 1. Synthesis of Compounds 1-38^a

^aReagents and conditions: (a) Ba(OH)₂·H₂O, EtOH, rt, 20 h, 19-97%; for preparation of **14**: NaOH, EtOH, 80 °C, 16 h, 38%; **15**: KOH, EtOH/H₂O (1/1), rt, 16 h, 95%; (b) Aqueous HCl, THF, rt, 16 h, 53-100%; (c) **32-33**: HCl, MeOH, rt, 2 h, 12-30%; **34**: aqueous HCl, H₂SO₄, rt, 16 h, DMF, 2%; (d) BBr₃, CH₂Cl₂, 0 °C to rt, 16 h, 10%; (e) Fe, aqueous HCl, EtOH, 80 °C, 2 h, 25%

In order to increase water-solubility of the target compounds, we planned to introduce a hydrophilic chain on ring B. Scheme 2 describes the synthesis of these modified chalcones. Treatment of 3,4-dihydroxybenzaldehyde in the presence of an excess of sodium hydride to deprotonate both hydroxyl groups and of an azido sulfonate led to alkylation at the more reactive 3-phenate site. Subsequent protection of the 4-hydroxyl moiety as a methoxymethyl ether gave compounds **39-41** that were condensed with *p*-chloroacetophenone as previously described.²⁸ Finally, MOM deprotection followed by Staudinger reduction of azides **42-44** in THF-water enabled the access to **45-47** as their hydrochloride salts.

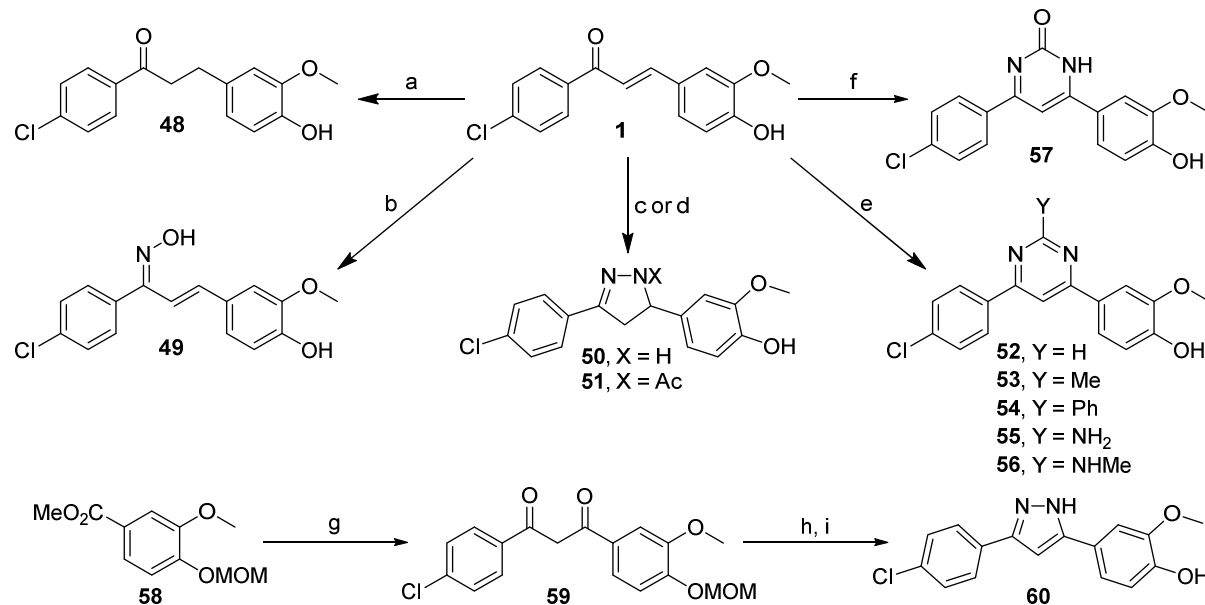
Scheme 2. Synthesis of Chalcones with Increased Water-solubility^a



^aReagents and conditions: (a) NaH, DMSO, Ts(OCH₂CH₂)_nN₃ for **39** and **40** or Ms(OCH₂CH₂)₃N₃ for **41**, 0 °C, 1 h, then rt, 16 h, 68-76%; (b) MOMCl, K₂CO₃, acetone, rt, 16 h, 95-100%; (c) 4-Cl-C₆H₄C(O)Me, Ba(OH)₂·H₂O, EtOH, rt, 4 h, 30-56%; (d) 12 M HCl, THF, rt, 16 h, 100%; (e) PS-PPh₃ for **45** and **46** or TCEP-HCl for **47**, THF/H₂O, rt, 16 h, 50-70%

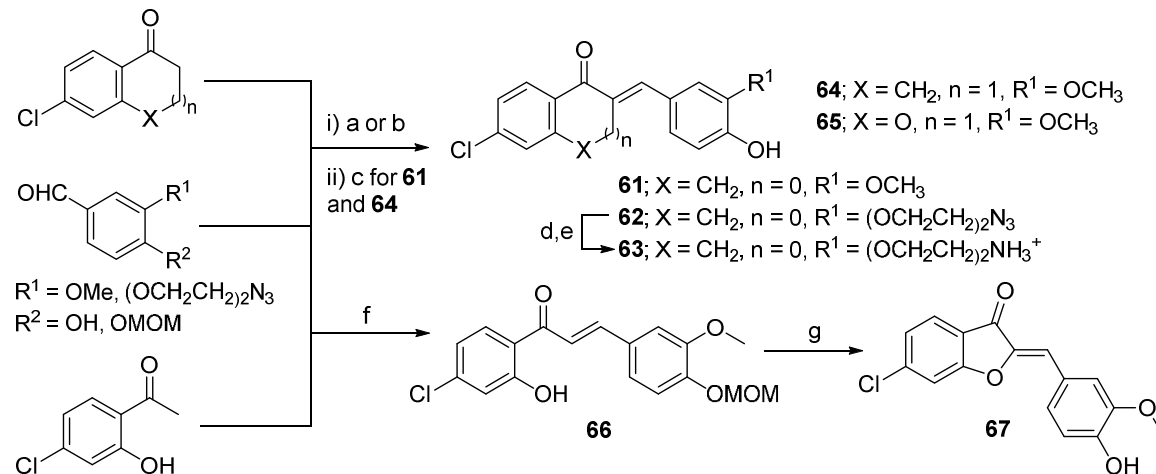
Several other analogues were prepared from **1** as shown in Scheme 3. Thus, 1,3-diarylpropan-1-one **48** was obtained by hydrogenation on platinum(IV) oxide and oxime **49** by reaction with hydroxylamine. Treatment with hydrazine hydrate in ethanol afforded the pyrazoline **50** or its *N*-acetyl analogue **51** when acetic acid was added to the reaction, both compounds being obtained as racemic mixtures. Several pyrimidines could be obtained by condensation of **1** either with imidamides (**52-54**), guanidines (**55-56**) or urea (**57**). The pyrazole **60** could be prepared by hydrazine hydrate treatment and MOM deprotection of diketone **59** prepared from 4-chloroacetophenone and MOM-protected methyl vanillate **58**.

Scheme 3. Synthesis of Compound 1 Derivatives with Central Core Modifications.^a



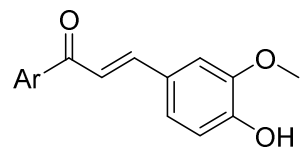
^aReagents and conditions: (a) PtO₂, H₂, EtOAc, rt, 20 min, 46%; (b) NH₂OH, pyridine, rt, 16 h, 43%; (c) NH₂NH₂·H₂O, EtOH, 80 °C, 4 h, 47%; (d) NH₂NH₂·H₂O, AcOH, EtOH, 80 °C, 18 h, 69%; (e) H₂N-CY=NH (Y = H, Me, Ph, NH₂, NHMe), DMF, base, 20-53%; (f) urea, HCl, dioxane/EtOH, 100 °C, 2 h, 43%; (g) NaH, 4-Cl-C₆H₄C(O)Me, THF, 0 °C, 1 h, 70 °C, 16 h, 32%; (h) NH₂NH₂·H₂O, EtOH, 80 °C, 10 h, 84%; (i) 12M HCl, THF, rt, 16 h, quant.

Constrained chalcones, incorporating an additional 5- or 6-membered ring, were also synthesized by reacting 6-chloro-3(2*H*)-benzofuranone, 6-chlorotetral-1-one and 7-chlorochroman-4-one with 4-hydroxy-3-methoxybenzaldehyde under the conditions already mentioned in Scheme 1. Due to the poor solubility of **61** in aqueous media, 6-chlorobenzofuran-1-one was reacted with benzaldehyde **40** bearing a hydrophilic ethylene glycol chain to provide after Staudinger reduction the more soluble compound **63**. Better solubility may also be obtained if the additional ring is an oxygenated heterocycle. We therefore prepared the benzofuran-3-one **67** by treating **66** with mercury(II) acetate in anhydrous pyridine (Scheme 4). All compounds were fully characterized by ¹H, ¹³C NMR and MS analysis and were obtained with a purity >95%.

Scheme 4. Synthesis of Conformationally Constrained Analogues^a

^aReagents and conditions: (a) Ba(OH)₂·H₂O, MeOH/EtOH, rt, 16 h, 28-48%; (b) SOCl₂, EtOH, 53-100%; (c) 12 M HCl, THF, rt, 16 h, quant.; (d) PS-PPh₃, THF/H₂O (4/1), 70 °C, 4 h, 20%; (e) 1 M HCl, rt, 30 min, quant.; (f) Ba(OH)₂·H₂O, EtOH, rt, 48 h, 28%; (g) Hg(AcO)₂, pyridine, 110 °C, 2 h, 25%

Structure-activity relationship and structural optimization. Pharmacomodulation of **1**, the first small organic compound-based chemokine neutraligand, led to a structure-activity relationship analysed in a systematic way by studying the consequences on CXCL12 binding of structural modifications of the 4-chloro aromatic ring (ring A; Table 1), of the phenolic part (ring B; Table 2) and of the central core of **1** (Table 3). Finally, rigid isosteres were prepared and tested to characterize the active conformation of **1** and to potentially improve its affinity and bioavailability (Table 4). The ability of each novel compound to inhibit CXCL12-CXCR4 interactions was carefully evaluated by using FRET-based binding experiments as previously described.^{18,29,30} In this assay, binding of Texas red-labeled CXCL12 (CXCL12-TR) to CXCR4 fused to EGFP expressed at HEK293 cell membrane induces fluorescence resonance energy transfer (FRET) between the EGFP and the Texas red, which can be monitored by the reduction of EGFP fluorescence emission at 510 nm. This reduction of EGFP fluorescence is dose-dependently inhibited by molecules that bind either CXCR4 or CXCL12 in a competitive manner.

Table 1. Effect of the Substituents of Ring A on CXCL12-TR Binding

Entry	Compd	Solubility ^a , μM	Ar	Inhibition of CXCL12-TR binding, K_i [nM]
1	1	>5	4-Cl-C ₆ H ₄ -	53 ± 31
2	2	>5	2-Cl-C ₆ H ₄ -	107 ± 35
3	3	>5	3-Cl-C ₆ H ₄ -	25 % of inhibition at 30 μM ^b
4	4	>5	4-F-C ₆ H ₄ -	430 ± 214
5	5	>5	4-Br-C ₆ H ₄ -	44 ± 17
6	6	>5	4-I-C ₆ H ₄ -	107 ± 17
7	7	>5	Ph-	>10 000
8	8	>5	4-Me-C ₆ H ₄ -	285 ± 17
9	9	>5	4-CF ₃ -C ₆ H ₄ -	1 070 ± 230
10	10	1.92	4- <i>i</i> -Pr-C ₆ H ₄ -	25 ± 10
11	11	0.95	2-naphthyl-	5% of inhibition at 30 μM ^b
12	12	>5	4-MeO-C ₆ H ₄ -	1 780 ± 714
13	13	>5	4-NO ₂ -C ₆ H ₄ -	30% of inhibition at 30 μM ^b
14	14	>5	4-HO ₂ C-C ₆ H ₄ -	5 350 ± 750
15	15	>5	4-HSO ₃ -C ₆ H ₄ -	6% of inhibition at 30 μM ^b
16	16	>5	2-F-4-Cl-C ₆ H ₃ -	107 ± 11
17	17	>5	2,3-Cl ₂ -C ₆ H ₃ -	357 ± 20
18	18	>5	2,4-Cl ₂ -C ₆ H ₃ -	48 ± 17
19	19	>5	2,5-Cl ₂ -C ₆ H ₃ -	53 ± 11
20	20	>5	2,6-Cl ₂ -C ₆ H ₃ -	71 ± 21
21	21	>5	3,4-Cl ₂ -C ₆ H ₃ -	714 ± 285
22	32	>5	3-Py-	> 10 000
23	33	>5	4-Py-	> 10 000

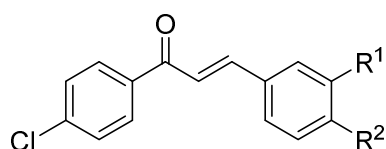
^aSolubility of compounds in HEPES-BSA buffer. ^bLimited by the solubility of the compound in HEPES-BSA buffer

Influence of ring A substitution on CXCL12 binding. The potency of series **1** analogues obtained by ring A modification to inhibit CXCL12-TR binding to the EGFP-tagged CXCR4 receptor (K_i) are listed in Table 1. The solubility of all compounds at a 5 μM concentration was validated before binding assessment. Interestingly, the unsubstituted phenyl derivative **7** is completely inactive at 10 μM (entry 7), indicating that the chalcone chemotype is not sufficient on its own for binding the chemokine, as

1
2
3 already reported.¹⁸ Substitution at position 4 with halogens results in a dramatic increase in affinity with
4 an optimum observed for chlorine (**1**) and bromine (**5**) with $K_i = 53$ nM and $K_i = 44$ nM, respectively
5
6 (entries 1 and 5). A two-fold decrease is observed with iodine (**6**) while a 4-fluoro substituent displays a
7
8 10-fold decrease in affinity (**4**) (entries 6 and 4). Chlorine and bromine may represent the best
9
10 compromise in terms of size, electronegativity and polarisability. The influence of position 4
11
12 substituents was further explored with limited success. Hence, methylation (**8**) provides a neutral ligand
13
14 with a $K_i = 430$ nM, whereas its electron withdrawing trifluoromethyl isostere **9** is even less potent ($K_i =$
15
16 1 070 nM) with an affinity comparable to the electron donating 4-methoxy derivative **12** ($K_i = 1$ 780
17
18 nM) (entries 8, 9 and 12). Interestingly, the hydrophobic and bulky 4-isopropyl group (**10**) further
19
20 improves the potency down to $K_i = 25$ nM (entry 10). However, its limited water solubility renders
21
22 difficult its further *in vivo* evaluation. Finally, a series of three compounds with electron withdrawing
23
24 substituents in position 4 were tested (**13**, **14** and **15**). None of them shows a significant affinity for
25
26 CXCL12 or CXCR4 (entries 13, 14 and 15). In summary, the chloro, bromo and isopropyl substituents
27
28 display the highest affinities, suggesting that bulkiness and polarisability are more important structural
29
30 determinants of activity than electron withdrawing or electron donating properties. The 3-chlorophenyl
31
32 analogue **3** shows a drastically reduced potency while the 2-chloro isostere **2** retains a good affinity ($K_i =$
33
34 107 nM), with only a two-fold decrease compared to **1**. The detrimental role of the 3-chloro substitution
35
36 is confirmed with the disubstituted compounds **17** and **21**: the 3,4-dichloro derivative **17** is indeed 14-
37
38 fold less potent than **11** while the 2,4-dichloro analogue **18** is equipotent ($K_i = 48$ nM) (entries 17, 11
39
40 and 18). The 2-fluoro-4-chloro compound **16** as well retains a significant potency ($K_i = 107$ nM) (entry
41
42 16). Similarly, if one compares the potency of the 2-chloro derivatives with a second chlorine in
43
44 positions 3, 5 and 6 (**17**, **19** and **20**, respectively), one observes the worst potency when a chlorine is in
45
46 position 3 and an affinity comparable to **1** for the 2,5-dichloro analogue **19** ($K_i = 53$ nM) (entries 17, 19
47
48
49
50
51
52
53
54
55

and 20). Noteworthy, the replacement of the phenyl moiety by a naphthyl (**11**), a 3- or a 4-pyridinyl (**32-33**) failed to provide active compounds (entries 11, 22 and 23).

Table 2. Effect of the substituents of ring B on CXCL12-TR binding



Entry	Compd	R ¹	R ²	Solubility ^a , μM	Inhibition of CXCL12-TR binding, K _i (nM)
1	1	-OMe	-OH	>5	53 ± 31
2	22	-OH	-OMe	>5	>10 000
3	23	-H	-H	1.17	18% of inhibition at 1 μM ^b
4	24	-OCH ₂ O-		2.31	25% of inhibition at 3 μM ^b
5	25	-OCH ₂ CH ₂ O-		>5	1 380 ± 357
6	26	-OMe	-H	0.36	>10 000
7	27	-OMe	-OMe	>5	>10 000
8	28	-OMe	-NO ₂	>5	>10 000
9	29	-H	-OH	>5	625 ± 3
10	30	-OEt	-OH	4.72	52% of inhibition at 5 μM ^b
11	34	-CO ₂ H	-OH	>5	>10 000
12	35	-OH	-OH	>5	350 ± 85
13	36	-OMe	-NH ₂	>5	>10 000
14	45	-OCH ₂ CH ₂ NH ₃ ⁺ Cl ⁻	-OH	>5	357 ± 121
15	46	-(OCH ₂ CH ₂) ₂ NH ₃ ⁺ Cl ⁻	-OH	>5	1 071 ± 321
16	47	-(OCH ₂ CH ₂) ₃ NH ₃ ⁺ Cl ⁻	-OH	>5	475 ± 71

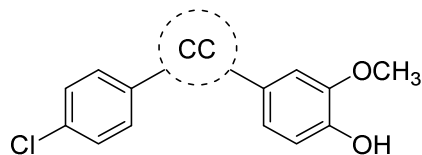
^a Solubility max of compound in HEPES-BSA buffer; ^b Limited by the solubility of the compound in HEPES-BSA buffer

Influence of ring B substitution on CXCL12 binding. In order to study the contribution of substitutions on ring B (Table 2), a series of analogues with a 4-chlorophenyl as ring A was synthesized. The water solubility of these analogues and their potency to inhibit the chemokine binding are listed in Table 2. Two ring B substituents are present in the original hit **1**: a methoxy group in position 3 and a hydroxyl in position 4. The derivative **23** with an unsubstituted aromatic ring B is only weakly active and has a low

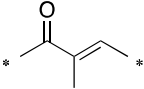
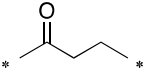
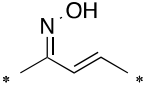
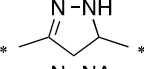
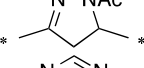
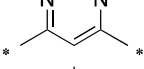
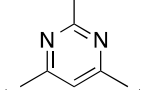
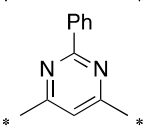
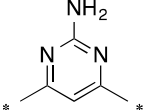
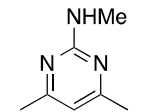
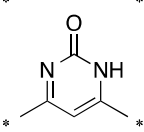
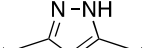
solubility in water (entry 2). When the methoxy group on ring B is absent (**22**), a ten-fold decrease in affinity is observed (entry 2) whereas a loss of affinity occurs when only the methoxy group is preserved (**26**) (entry 6). These findings suggest that the 4-hydroxy is more important than the 3-methoxy for the affinity towards CXCL12. When the hydroxyl and methoxy groups of **1** are inverted as in **22**, no activity is detected (entry 2). Compound **35** with a 3,4-dihydroxyphenyl ring B is almost two times more active than **29** bearing only a 4-hydroxyl group (entries 12 and 9). These results indicate that the presence and the position of the methoxy and hydroxyl substituents on ring B is crucial and contributes greatly to the affinity of compounds to CXCL12. Furthermore, when the hydroxyl group of **1** is replaced either by a methoxy (**27**), a nitro (**28**) or an amino group (**35**), the activity is very low (entries 7, 8 and 12). Accordingly, the cyclic dioxo analogues **24** and **25** are almost inactive (entries 4 and 5). These results clearly demonstrate the crucial role of the hydroxyl group at the 4 position on ring B.

In contrast, the nature of the R¹ alkoxy group can be fine-tuned without drastic loss of affinity (**30**) (entry 10). Thus, a 2-(polyethoxy)ethan-1-aminiium hydrophilic side-chain was introduced at this position to improve solubility properties, the best results being obtained with compounds **45** and **47** (entries 14 and 16).

Table 3. Effect of modification of central core (CC) on CXCL12-TR binding



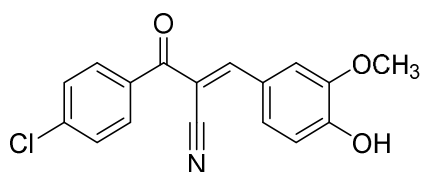
Entry	Compd	Central core	Solubility ^a , μM	Inhibition of CXCL12-TR binding, K _i (nM)
1	31		>5	> 10 000
2	37		2.6	> 10 000

3	38		>5	> 5 000
4	48		nd	> 10 000
5	49		>5	> 10 000
6	50		>5	107 ± 71
7	51		>5	> 10 000
8	52		4.29	30% of inhibition at 5 μM ^b
9	53		>5	1 680 ± 71
10	54		0.53	20% of inhibition at 0.3 μM ^b
11	55		>5	> 10 000
12	56		>5	> 10 000
13	57		>5	267 ± 71
14	60		19.5	> 10 000

^aSolubility of compounds in HEPES-BSA buffer; ^bLimited by the solubility of the compound in HEPES-BSA buffer

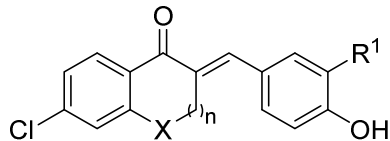
Influence of central part substitution and stiffening. Having determined the most suitable substituents on rings A and B, we next examined the influence of the central part of **1** on the affinity for CXCL12 (Tables 3 and 4). The reduction of the olefinic bond leads to the inactive compound **48** (Table 3, entry 4), likely due to the modification of both the electron distribution and the conformation of the molecule. The oxime **49**, the chalcone **31** where ring A and ring B have switched position or **37** and **38** with a

1
2
3 trisubstituted double bond have no significant activity on CXCL12 binding ($K_i > 5 \mu\text{M}$) (Table 3, entries
4
5 1, 2, 3 and 5). In our hands, only the α -cyano derivative (CN-Chalcone 4, Figure 2) retains a good
6
7 activity ($K_i = 53 \text{ nM}$). This compound was previously reported active *in vivo*, behaving as an antedrug
8
9 with potential therapeutic application.²⁹
10
11



12
13
14
15
16
17
18
19 **Figure 2.** Structure of the α -cyano derivative of CN-Chalcone 4.
20
21
22

23
24 **Table 4. Effect of Stiffening by Forming a 5- or 6-membered Ring Fused With Ring A on**
25 **CXCL12-TR binding**
26



Entry	Compd	X	n	R ¹	Solubility ^a , μM	Inhibition of CXCL12-TR binding, K_i (nM)
1	61	-CH ₂ -	0	-OMe	0.88	107 \pm 2
2	63	-CH ₂ -	0	-(OCH ₂) ₂ NH ₃ ⁺ Cl ⁻	>5	496 \pm 285
3	64	-CH ₂ -	1	-OMe	>5	70% of inhibition at 10 μM *
4	65	-O-	1	-OMe	>5	357 \pm 114
5	67	-O-	0	-OMe	>5	203 \pm 71

31
32
33
34
35
36
37
38
39
40 ^aSolubility of compounds in HEPES-BSA buffer
41
42
43
44
45
46
47
48
49
50
51
52
53
54
55
56
57
58
59
60

1
2
3 We then attempted to rigidify the central oxopropenyl moiety of **1** in two ways: 1) by building a 5- or 6-
4 membered heterocycle on this oxopropenyl connector (Table 3); 2) by bridging the *ortho* position of
5 ring A with C-2 of the oxopropenyl linker by one or two atoms (Table 4). In the first series, the
6 pyrazoline **50** is particularly interesting since it retains a good affinity ($K_i = 107$ nM) and shows that the
7 α,β -unsaturated ketone moiety is not mandatory in this case, compared to **48** (entries 4 and 6). The
8 acetylated derivative **51** however has a drastically reduced activity (entry 7). Surprisingly enough, the
9 pyrazole **60** is an inactive analogue though the conjugated system has been restored, thus showing the
10 subtlety of the docking of these molecules (entry 14). Conjugated six-membered ring analogues,
11 pyrimidines **52** to **56**, have a poor activity (entries 8 and 12). The simplest, unsubstituted pyrimidine **52**
12 shows a very modest inhibition (30%) at 5 μ M (entry 8). The activity is slightly improved by
13 substitution with a methyl (**53**) showing the possibility to reach a hydrophobic pocket (entry 9).
14 However, substitution by a phenyl group (**54**) or by the more polar amino groups (**55**, **56**) erases the
15 activity (entries 10-12). In contrast, the oxo analogue **57** retains a very significant activity ($K_i = 267$ nM)
16 though five-fold lower than **1** (entry 13). Noteworthy, **57** presents a more rigid core than **1** that freezes
17 the central chain in the all-*trans* conformation, indicating that this corresponds to the active
18 conformation of **1**. It is in agreement with crystal structures of both **1** and **57** that are very well
19 superimposable (Supplementary, Figure S1 and Tables S1 and S2). Interestingly, the pyrimidinone
20 nucleus in structure **57** is different from the overexploited chalcone chemotype. Furthermore, it contains
21 more heteroatoms than **1**, which results in an increased water-solubility (36 *versus* 9 μ M; Table 5, entry
22 5). As a consequence, **57** represents an interesting lead compound that was studied *in vivo* as detailed
23 below.
24
25
26
27
28
29
30
31
32
33
34
35
36
37
38
39
40
41
42
43
44
45
46
47
48
49
50
51
52
53
54
55
56
57
58
59
60

Table 5. Solubility and Stability of Selected Neutraligands

Entry	Compd	Solubility, ^a		Stability, ^b	
		μM		%	
		PBS	PBS/Cdx	PBS	PBS/Cdx
1	1	9	>300	100	100
2	6	1.2	319	100	100
3	45	4.2	>5 000	100	100
4	50	34.6	>3 000	78	98
5	57	36.4	>5 000	100	100
6	65	0.5	933	100	100
7	67	1.9	330	100	100

^aMeasured at pH 7.4 in PBS or PBS/Cdx, 24 h of incubation, 22 °C. ^bPercentage of remaining compound monitored by RP-HPLC after 24 h at 37 °C

The second series of rigidified compounds proved to be interesting as well (Table 4). Linking ring A with the α,β -unsaturated ketone via a methylene bridge as in benzofuranone **61** halves the activity ($K_i = 107$ nM) relative to **1** (entry 1). This two-fold decrease in affinity might stem from a higher hydrophobicity. Bridging with two methylene units as in tetralone **64** (entry 3) leads to a very low activity that may result from a less favorable conformation or from an excessive hydrophobicity. An oxy bridge leads to **67** that is slightly less active than **61** ($K_i = 203$ nM) but has a better water solubility (>5 μM vs 0.88 μM ; entries 1 and 5) whereas the oxymethylene derivative **65** is another less potent but still active compound ($K_i = 357$ nM; solubility >5 μM ; entry 4). In summary, two out of three rotatable bonds of the central core of compound **1** can be incorporated into rigid systems while retaining the ability to inhibit CXCL12 binding to its CXCR4 receptor in the nanomolar range. This supports the idea

1
2
3 that the active conformation of **1** is probably very close to its conformation in its crystal structure.
4
5 However, very subtle changes in the structure may lead to dramatic loss of activity, suggesting that this
6
7 series of ligands interacts with a well-defined and stringent binding site. At this point it was necessary to
8
9 demonstrate that these derivatives of molecule **1** are indeed neutraligands, that is to say that they
10
11 interfere with CXCL12-CXCR4 binding in actually binding to the chemokine and not to its receptor.
12
13
14
15
16

17 **Neutraligand characterization.** For the most potent compounds **6**, **45**, **50**, **57**, **65** and **67** arising from
18
19 the above SAR studies, confirmation of their neutralizing properties was achieved using the procedure
20
21 previously described (Figure 3).³¹ Briefly, using the FRET-based binding assay, the characterization of
22
23 CXCL12 neutraligands was evaluated in two conditions, differing by the sequence of addition of the
24
25 molecules. Hence, reduction of EGFP fluorescence emission is more pronounced when neutraligands are
26
27 preincubated (30 min) with the cells expressing CXCR4 receptor than when preincubated with CXCL12
28
29 prior to the addition to the cells, indicating that preliminary binding to the chemokine is the mechanism
30
31 of action, and the compounds are neutraligands and not receptor antagonists. Following this procedure
32
33 data obtained for all six compounds are consistent with a binding to the chemokine and not to the
34
35 receptor (Figure 3). Consequently, all selected compounds are indeed CXCL12 chemokine neutraligands
36
37 and behave as **1**.
38
39
40
41
42
43
44
45
46
47
48
49
50
51
52
53
54
55
56
57
58
59
60

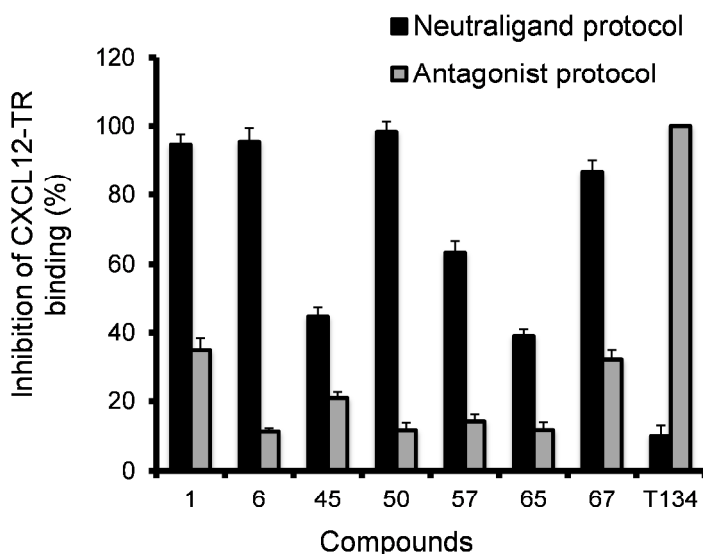


Figure 3. Inhibition of CXCL12-TR binding when neutraligands are incubated with the CXCR4-EGFP fused receptor-expressing cells prior to addition of CXCL12 (black bars; neutraligand protocol) or with CXCL12 prior to addition to CXCR4-EGFP fused receptor-expressing cells (grey bars; antagonist protocol). The compounds were tested at a concentration of $10 \times K_i$ (inhibition constant). The CXCR4 antagonist T134 (20 μM) was used as a control in both incubation protocols. Each column represents the mean (block) \pm SD (bars) of $n=3$ experiments.

***In vivo* evaluation of new neutraligands.** The six compounds identified as CXCL12 neutraligands were selected for *in vivo* studies. The iodo analogue **6** is slightly less potent than **1** *in vitro* ($K_i = 107$ nM vs 53 nM, respectively) but was selected since it may represent a valuable imaging probe for *in vivo* pharmacokinetic studies by single photon-emission computed tomography once I^{123} -radiolabeled. Compound **45** is a direct derivative of **1** branched with a water-solubilizing side chain. Compounds **50**, **57**, **65** and **67** are the most potent and soluble cyclic neutraligands identified *in vitro*, and are representative of four novel chemotypes: pyrazoline, pyrimidinone, benzofuranone and chromanone. First, their solubility in assay media was evaluated (Table 5). (2-Hydroxypropyl)- β -cyclodextrin (Cdx) was used as the excipient because of its low toxicity and capacity to increase the bioavailability of chemical compounds.³² Solubility studies in PBS/Cdx (10% w/w) showed that all compounds are

soluble at least at a 300 μM concentration (Table 5). The compound stability was evaluated in PBS or in PBS/Cdx. Only **50** was unstable in PBS, but the degradation could be avoided when Cdx was added (entry 4). Next, the *in vivo* activity of the selected compounds was evaluated in the 8-day murine model of allergic airway eosinophilic inflammation previously described (Figure 4A).^{21,33} Briefly, Balb/c mice were sensitized to ovalbumin (OVA) in presence of alum, and challenged 3 times at 24 h intervals with OVA in saline or saline alone. Treatment with each compound (300 nmol/kg in 10% PBS/Cdx) was administered by the intranasal route 2 h before each challenge. A bronchoalveolar lavage was performed 24 h after the last challenge, and inflammatory cell number quantified.³⁴

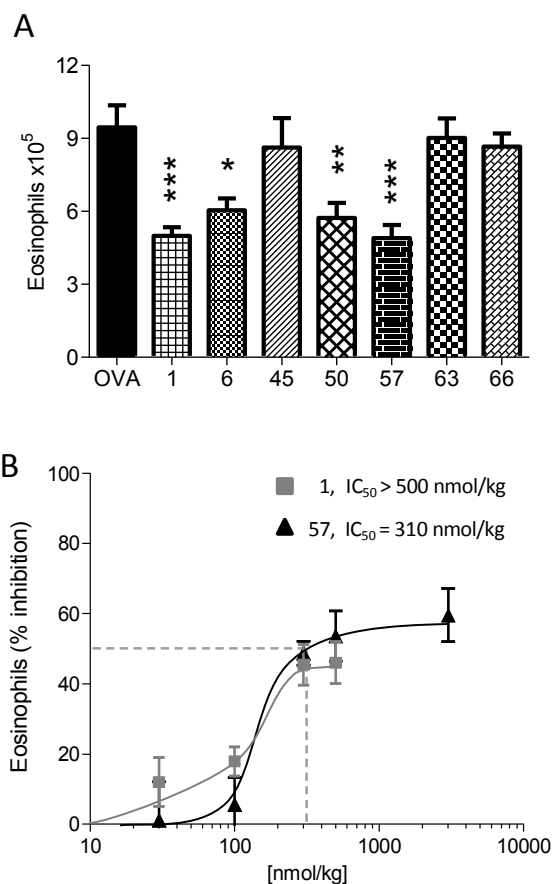


Figure 4. *In vivo* anti-inflammatory activity of CXCL12 neutraligands administered topically (i.n.) in the 8-day mouse model of allergic airway hyper eosinophilia. (A) Topical treatment with compounds **1**, **6**, **45**, **50**, **57**, **65** and **67** (300 nmol/kg) in PBS/CdX 10% (vehicle) administered 2 h before each allergen challenge. Absolute numbers of eosinophils, neutrophils, and lymphocytes in bronchoalveolar lavage

fluid (BAL) are shown. Blocks are means, and error bars are S.E.M. values ($n = 6/\text{group}$). Statistical analysis has been protected by a Bonferroni test. $^{\#}P \leq 0.05$ and $^{\#\#\#}P \leq 0.001$ vs. vehicle-treated saline group and $^*P \leq 0.05$, $^{**}P \leq 0.01$; $^{***}P \leq 0.001$ vs. vehicle-treated OVA group. (B) Dose-response effect of topical treatment with compounds **1** and **57** (i.n.). Compounds **1** (gray line) or **57** (black line) solubilized in PBS/Cdx 10% were administered 2 h before each allergen challenge. The percentage of inhibition of eosinophil recruitment in the bronchoalveolar lavage is shown. Data points are means and bars are SEM values ($n=6/\text{group}$).

Interestingly, despite a low solubility, the iodo-chalcone **6** retained a very good *in vivo* activity since it reduced eosinophil infiltration by 36% while the hit compound **1** reduced it by 47% at the same dose. Compounds **45**, **65** and **67** were almost inactive in our assay and were not further investigated. More interestingly, the two other rigidified analogues **50** and **57** that had similar *in vitro* potency displayed very good to excellent *in vivo* activity, inhibiting eosinophil infiltration by 39% and 48%, respectively (Figure 4A). Noteworthy, the recruitment of macrophages and lymphocytes was not affected by treatment with the CXCL12 neutraligands in this model, when neutrophil numbers were reduced with a trend towards significance (not shown). The chemical instability of **50** observed during both the synthesis and storage precluded the separation of both isomers and their further *in vitro* and *in vivo* evaluation. We therefore decided to select **57** as lead neutraligand, and characterized its activity (IC_{50}) *in vivo* in a dose-response efficacy study *versus* **1** on eosinophil recruitment in our mouse model. The IC_{50} of the reference compound **1** could not be determined precisely because the solubility threshold was reached at 500 nmol/kg even when solubilized in PBS/Cdx. In contrast, the soluble novel pyrimidinone **57** gave an IC_{50} calculated as 310 nmol/kg (Figure 4B).

We thereafter characterized further 1) the Michael-acceptor reactivity of **57**, 2) its binding properties to CXCL12, and 3) its selectivity towards other chemokines.

Michael-Acceptor Reactivity. The Michael-acceptor character of **57** and **1** was evaluated in the

1
2
3 presence of glutathione (GSH, 2.5 eq). As determined by LC-MS analysis, after 2 h at 37 °C, more than
4
5 30% of **1** were converted into the GSH-**1** adduct while **57** was found much more stable without any
6
7 formation of GSH-**57** adduct (Supplementary, Figure S2).
8
9

10
11
12 **Biophysical characterization.** To support the neutraligand character of **57** reported above from FRET-
13
14 based binding assay, the binding to CXCL12 was examined by monitoring changes in its emission of
15
16 tryptophan fluorescence intensity (Figure 6). Indeed, as previously reported, CXCL12 contains a single
17
18 tryptophan residue (Trp-57) whose intrinsic fluorescence can be modulated by neutraligands.¹⁸ Thus, we
19
20 observed that tryptophan fluorescence intensity at 340 nm (excitation at 285 nm) declined monotonically
21
22 when CXCL12 (2 μM) was incubated with increasing concentrations of **57** (Figure 6C). The resulting
23
24 tryptophan fluorescence inhibition curve was satisfactorily fitted according to a 1:1 stoichiometry
25
26 interaction mode and the deduced dissociation constant ($K_d = 780 \pm 320$ nM) was in the same range than
27
28 that determined by FRET-based assay ($K_i = 267 \pm 71$ nM).
29
30
31

32
33 As a control from the whole strategy, the structurally close pyrimidinone **68** (Figure 5A) was
34
35 synthesized (supplementary for the synthesis) and tested in the FRET-based assay described above
36
37 (Figure 5B). Thereby, **68** inhibited CXCL12 binding to CXCR4 by less than 5% at 300 μM. In the
38
39 tryptophan fluorescence assay, **68** non-specifically decreased Trp fluorescence intensity at 340 nm
40
41 (Figure 5C). Additionally, **68** was inactive in the mouse model of allergic airway eosinophilic
42
43 inflammation at 300 nmol/kg (data not shown).
44
45
46
47
48
49
50
51
52
53
54
55
56

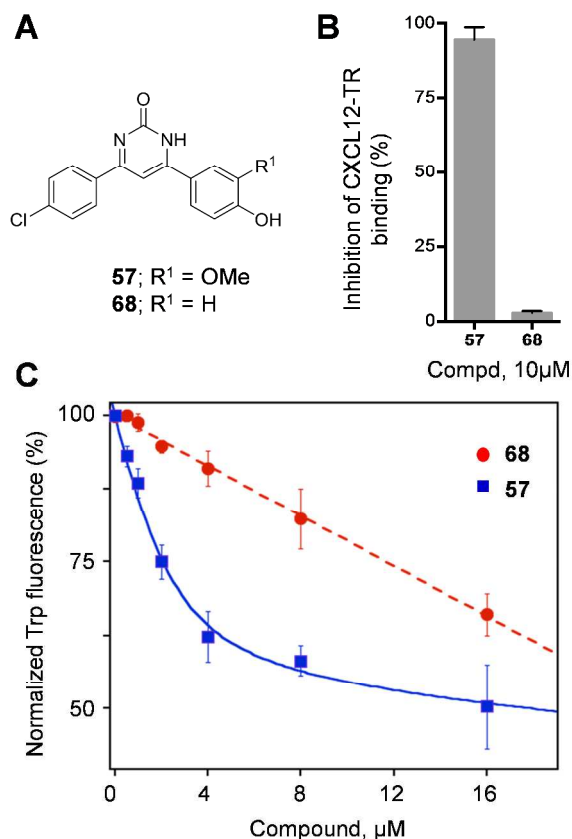


Figure 5. Interaction between **57** and CXCL12. (A) Chemical structure of pyrimidinone **68** as compared to **57**. (B) Inhibition of CXCL12-TR binding when **57** and **68** (10 μM) are incubated with the CXCL12 chemokine prior to addition to CXCR4-EGFP fused receptor-expressing cells. (C) Titration of binding of pyrimidinones **57** (squares) and **68** (circle) to CXCL12 determined by monitoring changes in the maximal emission of Trp fluorescence of CXCL12 (measured at 340 nm). Increasing amounts of molecule were added to CXCL12 solution (2 μM in HEPES buffer). The equation used to fit experimental data is the root of the second order equation: $(RL)^2 + (RL) \times (-R_0 - L_0 - K_D) + R_0 \times L_0 = 0$ where $(RL) = ((R_0 + L_0 + K_D) \pm ((-R_0 - L_0 - K_D)^2 - 4 \times R_0 \times L_0)^{1/2})/2$ and where R_0 , the concentration of chemokine, is set to 2 μM; L_0 is the initial concentration of molecule; K_D is the dissociation constant of molecule for the chemokine; and RL is the fractional concentration of receptor and ligand complex. Data are means (dots) and SD (bars) values of three independent experiments.

1
2
3 **Molecular modeling of compounds 1 and 57 bound to CXCL12.** Physicochemical properties as well
4 as the herein presented structure-activity relationship suggest a common binding mode of compounds 1
5 and 57 to CXCL12 that completely differs from that observed with the inhibitor recently described.²⁴
6
7
8
9
10 The later compound is bound to the wide and accessible pocket, which is incompatible with the
11 observed nanomolar binding affinities of our neutral ligands. We therefore envisaged the possibility of an
12 alternative and mostly apolar pocket that would be just large enough to tightly host compounds 1 or 57.
13
14 Systematic scanning of the CXCL12 chemokine dimeric structure²⁴ with the in-house developed VolSite
15 program³⁵ clearly indicates the presence of a small but structurally druggable pocket (Figure 6A) at the
16 vicinity of Trp57, whose importance to compound 1 binding has previously been evidenced by
17 fluorescence spectroscopy.¹⁸ Docking of compounds 1 and 57 to this pocket is possible at the condition
18 to allow side chain flexibility for three residues (Arg20, Trp57 and Tyr61, Figure 6) that would control
19 the entry to the Trp57 pocket. Two independent docking algorithms, Plants,³⁶ and Surflex-Dock³⁷ agree
20 to similarly dock both compounds in a manner that is almost fully consistent with the herein described
21 structure-activity relationships, assuming a common binding mode for compounds 1 and 57 (Figure
22 6B,C). First, the 4-chlorophenyl ring A is deeply buried in an apolar subpocket (Val23, Leu26, Trp57)
23 whose size is nicely complementary to that of a 4-chlorophenyl substituent. The observed lower affinity
24 of the 3-chlorophenyl analog 3 can be easily explained by close proximity of Leu26 or Trp57 backbone
25 atoms that would prevent a complete entry into the pocket. Second, the proposed binding mode also
26 explains the crucial role of a 4-hydroxyphenyl ring B. The aromatic ring is stacked between Pro32 and
27 the ammonium moiety of Lys64 to which a π -cation interaction is observed in our model. The hydroxyl
28 group in ring B donates a hydrogen bond to the nearby Gln37 side chain, thereby explaining the higher
29 affinity of the hydroxyle with respect to the methoxy analog. Third, the ketone moiety of compound 1 is
30 hydrogen-bonded to Arg20 side chain (Figure 6C). In case of compound 57, the bioisosteric pyrimidin-

2(1H)-one core is ideally located to accept a bidentate hydrogen bond from Arg20 side chain (Figure 6B). Contrarily to compound **57**, compound **1** is predicted to adopt another possible binding mode (Figure 6D) in which positions of aromatic rings A and B had been interchanged, the ketone being still anchored to Arg20. Depending on the substituents at rings A and B, the binding mode may readily switch from one to the other possible orientations.

In the proposed binding mode, the absolute binding free energy of compounds **1** (preferred binding mode) and **57**, computed by the Hyde scoring function,³⁸ is estimated to $-18.60 \text{ kJ.mol}^{-1}$ and $-14.92 \text{ kJ.mol}^{-1}$, close to the experimentally observed values of -17.78 and $-16.06 \text{ kJ.mol}^{-1}$, respectively.

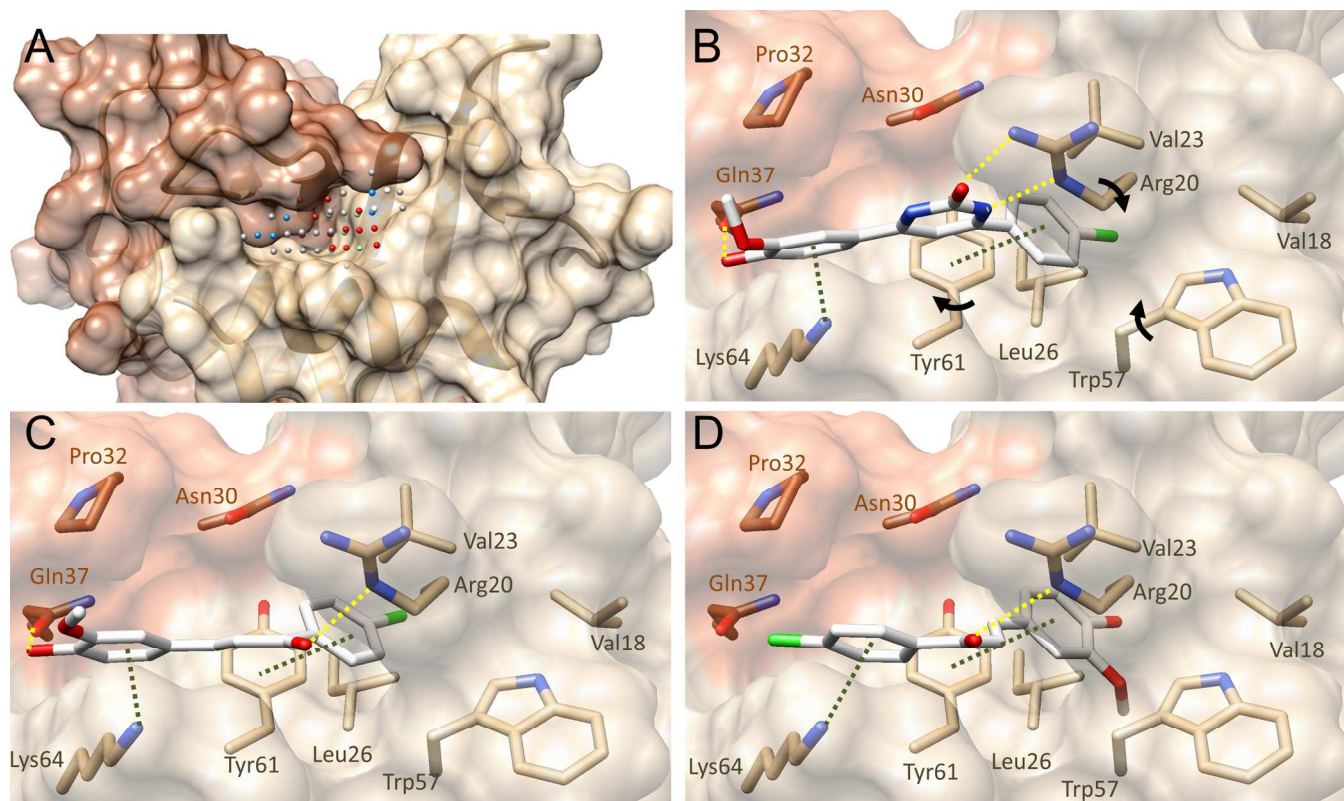


Figure 6. Hypothesized binding mode of compounds **1**, **57** to the CXCL12 homodimer. The two monomers are displayed by a transparent surface and backbone ribbons (monomer 1, tan; monomer 2, sienna). (A) Detection of a druggable cavity (colored spheres) nearby Trp57 at the surface of the CXCL12 homodimer (PDB ID 4UAI). The volume of the cavity, detected by VolSite³⁵ is 184 \AA^3 . Cavity

1
2
3 points are colored by pharmacophoric properties (red, hydrogen bond acceptor; blue, hydrogen bond
4 donor; gray, hydrophobic/aromatic). (B) PLANTS docking pose of compound **57** to CXCL12. Three
5 side chains (indicated by an arrow) are allowed to freely move, thereby widening the pocket volume up
6 to 371 Å³. Hydrogen bonds are indicated by yellow broken lines. Aromatic and π -cation interactions are
7 represented by dark green broken lines. Residues contributing to the binding cavity are labelled at their
8 C- α atom (tan, monomer 1; sienna, monomer B). (C) PLANTS preferred docking pose of compound **1** to
9 CXCL12. (D) PLANTS alternative docking pose of compound **1** to CXCL12.
10
11
12
13
14

15 **Binding selectivity towards other chemokines.** The selectivity of **57** was evaluated towards four other
16 chemokines, namely CCL17, CCL22, CCL5 and CCL2 by using the neutraligand protocol of the
17 recently reported Time-Resolved Intracellular Calcium recording (TRIC-r) assay³⁹ (Figure 7). This
18 generic assay enables the discovery of chemokine neutralizing molecules (neutraligands) by
19 differentiating them from molecules that block the receptor (antagonists). Initially described for the
20 identification of CCL17 and CCL22 neutraligands, the assay has been set-up for CXCL12.³⁹ Thereby, as
21 depicted in Figure 7, pyrimidinone **57** at 10 μ M is able to inhibit the increase in intracellular calcium
22 concentration in EGFP-CXCR4⁺ HEK cells in response to CXCL12, while it has no effect on calcium
23 responses triggered by either CCL17 or CCL22 on EGFP-CCR4⁺ HEK cells, CCL5 on EGFP-CCR5⁺
24 HEK cells, or by CCL2 on EGFP-CCR2⁺ HEK cells. These results demonstrate the high selectivity of
25 **57** towards CXCL12 vs other chemokines also involved in asthma.
26
27
28
29
30
31
32
33
34
35
36
37
38
39
40
41
42
43
44
45
46
47
48
49
50
51
52
53
54
55
56
57
58
59
60

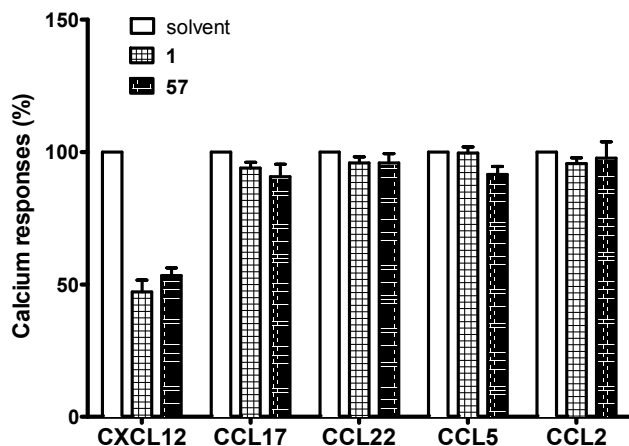
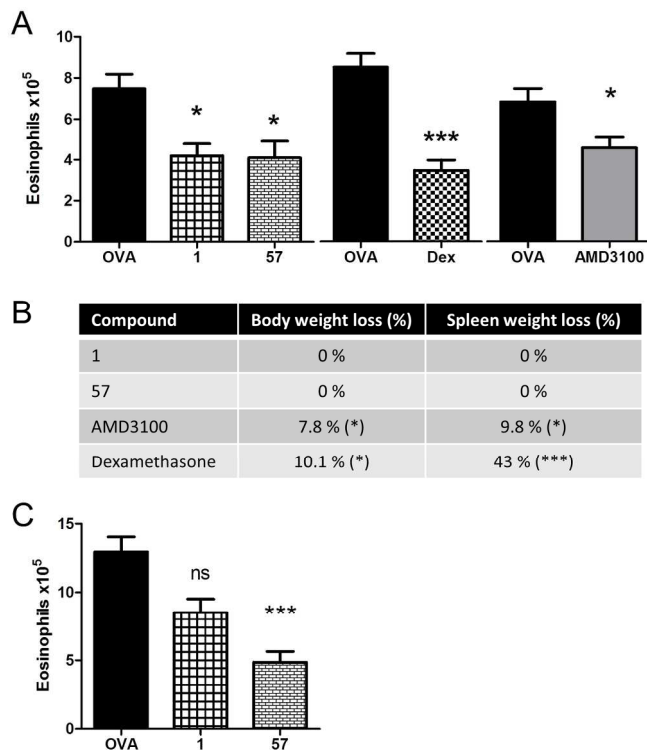


Figure 7. Selectivity of compounds **1** and **57** towards 5 chemokines. Effect of DMSO (white bars) and compound **1** or **57** (10 μ M) on calcium responses triggered by either 5nM CXCL12 on EGFP-CXCR4⁺ HEK cells, by 5nM CCL17 and CCL22 on EGFP-CCR4⁺ HEK cells, 5nM CCL5 on EGFP-CCR5⁺ HEK cells, or by 5nM CCL2 on EGFP-CCR2⁺ HEK cells. Each column represents the mean (block) \pm SD (bars) of n=3 experiments.

***In vivo* evaluation of neutraligand **57** activity and safety.** At this stage of the study, pyrimidinone **57** turned out to be a CXCL12-selective neutraligand with markedly improved solubility and no longer Michael acceptor character. In addition, we demonstrated its anti-inflammatory activity at low dose after local administration in a murine model of allergic airway hyper eosinophilia. These results prompted us to further evaluate **57** *in vivo*. We first compared the activity and safety of compounds **1** and **57** versus the main commercialized comparators, the CXCR4 antagonist AMD3100 and the glucocorticoid dexamethasone (Dex) in the mouse model of hyper eosinophilia. The compounds were administered i.p. 2 h before the allergen challenge. Neutraligands **1** and **57** (350 μ mol/kg) inhibited eosinophil infiltration by 54 and 55%, and AMD3100 (12.6 μ mol/kg) and Dex (2.5 μ mol/kg) by 33 and 59%, respectively (Figure 8A). The anti-inflammatory activity of AMD3100 and Dex was accompanied with a statistically reliable decrease in body and spleen weight, indicating major adverse event-related perturbation by these compounds. In contrast, neutraligands **1** and **57** did not exhibit any side effects (Figure 8B). Even after

1
2
3 10 daily administrations of neutraligands **1** or **57**, no weight loss was observed (Figure 8B) or other
4 signs of toxicity, prostration, bristly hair (not shown), which ascertains that our two neutraligands are
5 safe. This result was confirmed by the absence of lesion in our Gomori's staining histological studies of
6 liver, spleen, heart and kidney (Supplementary Figure S3). In addition, our experiment shows the anti-
7 asthma activity of the CXCR4 antagonist AMD3100 in our model of allergic airway hypereosinophilia,
8 in a same potency as reported in a model of cockroach-induced asthma.⁴⁰ Altogether, these results
9 confirm that the prevention of the interaction between CXCL12 and CXCR4 axis by our CXCL12
10 neutraligands could be a beneficial and safe strategy for asthma treatment. Finally, we evaluated the oral
11 activity of our novel neutraligand **57**, which could be an interesting additional approach for asthma
12 treatment. We investigated the oral activity of the CXCL12 neutraligands **1** and **57** administered by
13 gavage (1400 $\mu\text{mol/kg}$) as assessed in the same murine model of hypereosinophilia (Figure 8C).
14 Neutraligand **57** shows a large and statistically reliable inhibition of eosinophil recruitment (62%
15 inhibition), whereas compound **1** only exhibited a trend towards inhibition. Therefore, **57** is reported as
16 the first orally active CXCL12 neutraligand in this model of asthma.
17
18
19
20
21
22
23
24
25
26
27
28
29
30
31
32
33
34
35
36
37
38
39
40
41
42
43
44
45
46
47
48
49
50
51
52
53
54
55
56
57
58
59
60



28
29
30
31
32
33
34
35
36
37
38
39
40
41
42
43
44
45
46
47

Figure 8. Anti-inflammatory activity of CXCL12 neutraligands in a mouse model of allergic eosinophilic airway inflammation. (A) Effect of systemic (i.p.) treatment with compounds **1** and **57** compared to the glucocorticoid dexamethasone (Dex) and the CXCR4 antagonist AMD3100 (Plerixafor) in the 8-day mouse model of allergic airway hyper-eosinophilia. Neutraligands **1** and **57** (350 $\mu\text{mol/kg}$ in PBS/CMC 1%), dexamethasone (2.5 $\mu\text{mol/kg}$) or AMD3100 (12.6 $\mu\text{mol/kg}$) were administered intraperitoneally 2 h before each challenge. Absolute numbers of eosinophils in BAL fluid are shown. Blocks are means, and error bars are S.E.M. values ($n = 6/\text{group}$). (B) Side effects of treatment with compounds **1** and **57** compared to Dex and AMD3100 measured on body and spleen weight loss in the model here above (24h after three daily administrations). (C) Effect of oral treatment with compounds **1** and **57** in the 8-day mouse model of hyper-eosinophilia. Compounds in PBS/MC 0.5%/Tween 80 0.05% (1400 $\mu\text{mol/kg}$) were administered intraperitoneally 2 h before each allergen challenge. Absolute numbers of eosinophils in BAL fluid are shown. Blocks are means, and error bars are S.E.M. values ($n = 6/\text{group}$). Statistical analysis has been protected by a Bonferroni test. * $P \leq 0.05$, *** $P \leq 0.001$ in comparison with vehicle-treated OVA group.

48
49
50
51
52
53
54
55
56
57
58
59
60

Thereby, pyrimidinone **57** herein reported is a novel neutraligand able to bind selectively CXCL12 and to inhibit CXCL12-CXCR4 interaction. As compared to hit compound **1**, pyrimidinone **57** displays an

1
2
3 improved solubility and chemical stability. Finally, neutraligand **57** inhibits allergic eosinophilic airway
4
5 inflammation in mice when administered orally or locally.
6
7
8
9

10 CONCLUSION

11
12 We and others previously demonstrated that it is possible to identify small non-peptidic molecules able
13
14 to bind chemokines and prevent their binding to chemokine receptors, thus neutralizing their function.
15
16 ^{18,21,22,35} Such molecules were termed neutraligands due to their ability to neutralize a ligand, the
17
18 chemokine, and to prevent interaction with its target receptor. We already reported CXCL12
19
20 neutraligands administered as prodrugs²¹ or antedrug neutraligands²² with *in vivo* potential at inhibiting
21
22 airway eosinophilic inflammation. However, these compounds display major drawbacks for drug
23
24 development such as owning a Michael acceptor type scaffold limiting its potential in drug
25
26 development. To overcome these limitations, we explored herein the structure-activity relationship
27
28 around the first CXCL12 neutraligand **1**.¹⁸ Pharmacomodulation opportunities on the three parts of the
29
30 molecule were explored. 4-Chloro or 4-isopropyl are the most potent substituents on the acylated phenyl
31
32 ring of the chalcone backbone. Interestingly, the iodo analogue compound **6** retained *in vitro* and *in vivo*
33
34 activity that might be exploited in the future for radioimaging studies. We also identified that the 3-
35
36 methoxy-4-hydroxy combination pattern remained the most efficient one on the other phenyl ring of the
37
38 chalcone motif with very little freedom for pharmacomodulation. The central core of the molecule is
39
40 very sensitive to any structural change. Interestingly, it was possible to move away from the chalcone
41
42 backbone by rigidifying the flexible and thiol reactive α,β -unsaturated ketone by incorporation in cyclic
43
44 systems. Thereby, a pyrazoline and a pyrimidinone derivatives were found to behave as novel CXCL12
45
46 neutraligands with affinities in the 100 nM range *in vitro* and a significant *in vivo* activity in a model of
47
48 allergic eosinophilic airway inflammation. To summarize, pyrimidinone **57** is a valuable analog of **1** for
49
50
51
52
53
54
55
56

31

1
2
3 further *in vivo* studies of CXCL12 implication in *in vitro* and *in vivo* models. Its slightly reduced
4
5 intrinsic affinity for CXCL12 is largely compensated for by enhanced chemical and biological stabilities
6
7 and physicochemical properties that allow improved *in vivo* potency in the murine model of
8
9 hypereosinophilia. In particular, **57** is no longer a Michael acceptor. This therefore allows to rule out
10
11 covalent labelling of CXCL12 as the mechanism of action of **1** and its chalcone derived analogs. In
12
13 addition, **57** is more soluble and therefore more potent at reducing eosinophil recruitment, which is
14
15 attained at very low doses after i.n. administration ($IC_{50} = 300$ nmol/kg, i.e. 100 μ g/kg) in the murine
16
17 model of allergic eosinophilic asthma. In addition, **57** is the first orally active CXCL12 neutraligand,
18
19 exhibiting anti-inflammatory activity when administered *per os*. Altogether, these results demonstrate
20
21 that **57** represents a stable, selective, locally and orally active pharmacological tool to investigate the
22
23 physiological and pathophysiological functions associated with the CXCL12-CXCR4 axis, and a first
24
25 step on the route towards the development of anti-inflammatory and novel anti-asthma drugs.
26
27
28
29
30
31
32
33
34
35
36
37
38
39
40
41
42
43
44
45
46
47
48
49
50
51
52
53
54
55
56
57
58
59
60

EXPERIMENTAL PROCEDURES

Material and Methods

Chemistry

Reagents were obtained from commercial sources and used without any further purification. Thin-layer chromatography was performed on silica gel 60F₂₅₄ plates. Flash chromatography was performed on silica gel cartridges (SiliaSep Flash cartridges silica, 40-63 μm) or RP18 prepacked columns (PuriFlash 30 μm , Interchim) prepacked columns using a Spot II Ultimate apparatus from Armen Instrument. Semi-preparative RP-HPLC were performed on one of the following columns: SunFire C18 OBD (5 μm , 19x150 mm, Waters) or SymmetryShield RP 18 (7 μm , 19x300 mm, Waters) on PLC2020 from Gilson using MeCN – 0.1% TFA/water – 0.1% TFA gradient (flow rate: 15 mL/min) unless otherwise specified.

¹H and ¹³C NMR spectra were recorded on a Bruker 400 MHz/100 MHz, 300 MHz/75 MHz and 200 MHz/50 MHz spectrometer. Conditions are specified for each spectrum (temperature 25 °C unless specified). Chemical shifts are reported in parts per million (ppm) relative to residual solvent and coupling constants (*J*) are reported in hertz (Hz). Signals are described as s (singlet), d (doublet), t (triplet), q (quartet), m (multiplet), dd (doublet of doublets), dt (doublet of triplets), dq (doublet of quadruplets) and br s (broad singlet).

Analytical HPLC analyses were performed on an Agilent 1000 series apparatus, equipped with an Ascentis Express C18 column (2.7 μm , 4.6x7.5mm) under the following conditions: flow rate: 1.6 mL/min; buffer A: 0.1% aqueous TFA, buffer B: 0.1% TFA in CH₃CN; 5-95% buffer B over 7 min; detection: $\lambda = 220/254$ nm. For each compound, HPLC purity was $\geq 95\%$. LC/MS spectra were obtained on an Agilent HPLC single quadrupole spectrometer (1200RRLC/1956b-SL) equipped with a THERMO Hypersyl column (1.9 μm , 1x30 mm) using an Agilent Multimode ion source. HRMS spectra were

1
2
3 obtained on an Accurate-Mass Q-TOF spectrometer from Agilent using electrospray ionisation (ESI).
4
5 Infrared (IR) spectra were recorded in inverse wavenumbers (cm^{-1}) on a Thermo Nicolet 380 FT-IR
6
7 spectrometer. The melting points of the solid compounds were measured with a Büchi B-540.
8
9

10
11
12 **Chalcone synthesis under basic conditions - General procedure A.** To a solution of the desired
13
14 substituted benzaldehyde (2.00 mmol, 1.0 equiv) and acetophenone (2.00 mmol, 1.0 equiv) derivative in
15
16 EtOH (5 mL), was added $\text{Ba}(\text{OH})_2 \cdot \text{H}_2\text{O}$ (4.00 mmol, 2.0 equiv). The reaction was stirred at rt. After
17
18 completion of the reaction, the mixture was evaporated under reduced pressure. Water was added to the
19
20 residue and the mixture was extracted three times with EtOAc or CH_2Cl_2 . The combined organic layers
21
22 were dried over anhydrous sodium Na_2SO_4 , filtered and concentrated. Purification on a silica gel column
23
24 or semi-preparative HPLC afforded the desired product.
25
26
27
28
29

30
31 **Methoxymethylation of phenol - General procedure B.** To a solution of a phenol derivative (1.50
32
33 mmol, 1.0 equiv) in anhydrous MeCN or DMF (2 mL), were added K_2CO_3 (3.00 mmol, 2.0 equiv) and
34
35 methoxymethyl chloride (2.25 mmol, 1.5 equiv). The mixture was stirred overnight at rt. After removal
36
37 of the solvent under reduced pressure, water was added to the residue and the aqueous layer was
38
39 extracted 3 times with EtOAc or CH_2Cl_2 . The combined organic layers were dried over anhydrous
40
41 Na_2SO_4 , filtered and concentrated to afford the desired compound without purification.
42
43
44
45
46

47 **Deprotection of methoxymethyl ether - General procedure C.** To a solution of a methoxymethyl
48
49 ether derivative (1.00 mmol) in THF (5 mL) was added concentrated aqueous HCl (8 drops). The
50
51 mixture was allowed to stir overnight at rt and was then evaporated to afford the desired compound.
52
53 Purification on a silica gel column or by semi-preparative RP-HPLC was performed if necessary.
54
55

(E)-1-(4-Chlorophenyl)-3-(4-hydroxy-3-methoxyphenyl)prop-2-en-1-one (1). To a solution of 4-hydroxy-3-methoxybenzaldehyde (4.92 g, 32.34 mmol) and 1-(4-chlorophenyl)ethan-1-one (5.0 g, 32.3 mmol) in EtOH (16 mL) at 0 °C, was slowly added SOCl₂ (1.650 mL, 22.75 mmol). The mixture was allowed to warm to rt and was stirred overnight. Water was added to the solution and the mixture was extracted 2 times with CH₂Cl₂. The combined organic layers were dried over anhydrous Na₂SO₄, filtered and concentrated. The solid was recrystallized from EtOH to give a yellow solid (7.368 g, 25.49 mmol, **79%**). **¹H NMR** (400 MHz, MeOD-*d*₄) δ 8.05 (d, *J* = 8.6 Hz, 2H), 7.74 (d, *J* = 15.5 Hz, 1H), 7.56 (d, *J* = 15.5 Hz, 1H), 7.52 (d, *J* = 8.6 Hz, 2H), 7.35 (d, *J* = 2.0 Hz, 1H), 7.21 (dd, *J* = 8.2 Hz, *J* = 2.0 Hz, 1H), 7.17 (d, *J* = 1.9 Hz, 1H), 6.84 (d, *J* = 8.2 Hz, 1H), 3.93 (s, 3H); **¹³C NMR** (100 MHz, CDCl₃) δ 191.2, 151.6, 149.6, 147.8, 140.2 (2C), 138.4, 131.3, 130.1, 128.3, 125.4, 119.5, 116.8 (2C), 112.4, 56.7; **HRMS** (ESI-TOF): calcd for C₁₆H₁₄ClO₃ [M+H]⁺: 289.06260, found: 289.06356; **mp** 113-115 °C; **IR** (Neat) 3505, 1650, 1577, 1509, 1432, 1272, 1215, 1158, 1027, 979, 817, 505, 474 cm⁻¹.

(E)-3-(4-Hydroxy-3-methoxyphenyl)-1-(4-iodophenyl)prop-2-en-1-one (6). General procedure A, from 1-(4-iodophenyl)ethan-1-one (251 mg, 1.02 mmol) and 3-methoxy-4-(methoxymethoxy)benzaldehyde (200 mg, 1.02 mmol), **46%** yield, then general procedure C, quantitative yield. **¹H NMR** (400 MHz, CDCl₃) δ 9.73 (br s, 1H), 7.93 (ABq, 4H, Δδ_{AB} = 0.05, *J*_{AB} = 8.6 Hz), 7.70 (ABq, 2H, Δδ_{AB} = 0.03, *J*_{AB} = 15.3 Hz), 7.51 (d, *J* = 2.0 Hz, 1H), 7.28 (dd, *J* = 8.3, 2.0 Hz, 1H), 6.83 (d, *J* = 8.3 Hz, 1H), 3.87 (s, 3H); **¹³C NMR** (100 MHz, CDCl₃) δ 188.4, 149.9, 148.0, 145.4, 137.6 (2C), 137.2, 130.1, 126.1, 124.3, 118.2, 115.6 (2C), 111.8, 101.3, 55.8; **HRMS** (ESI-TOF): calcd for C₁₆H₁₄IO₃ [M+H]⁺: 380.99822, found: 380.99852; **mp** 134-136 °C; **IR** (Neat) 3341, 1644, 1572, 1549, 1515, 1233, 1209, 1058, 1026, 1004, 817, 738 cm⁻¹; **HPLC** *t*_R = 5.61 min, purity > 97% (254 nm).

3-(2-Azidoethoxy)-4-(methoxymethoxy)benzaldehyde (39).

Step 1 – Coupling with PEG chain: NaH (817 mg, 20.4 mmol, 60% w/w in oil) was suspended in anhydrous toluene (10 mL). Magnetic stirring was stopped after 5 min. After decantation, toluene was removed. Anhydrous DMSO (28 mL) and 3,4-dihydroxybenzaldehyde (1.69 g, 12.2 mmol) were added and the mixture was allowed to warm at 25 °C for 1 h. 2-azidoethyl 4-methylbenzenesulfonate (2.47 g, 10.2 mmol) in anhydrous DMSO (5 mL) was added slowly and the mixture was stirred overnight at rt. The reaction was poured into 100 mL of ice-water and neutralized with 1 M aqueous HCl. The mixture was extracted 3 times with EtOAc. The combined organic layers were washed with brine, dried over anhydrous Na₂SO₄, filtered and concentrated. Purification on silica gel eluting with 5-100% MeCN adding 0.1% TFA in water and freeze-drying afforded 3-(2-azidoethoxy)-4-hydroxybenzaldehyde as a white powder (1.54 g, 7.43 mmol, **68%**). ¹H NMR (400 MHz, CDCl₃) δ 9.80 (s, 1H), 7.45 (d, *J* = 8.1 Hz, 1H), 7.41 (s, 1H), 7.06 (d, *J* = 8.1 Hz, 1H), 6.32 (br s, 1H), 4.29 (t, *J* = 4.9 Hz, 2H), 3.68 (t, *J* = 4.9 Hz, 2H); ¹³C NMR (100 MHz, CDCl₃) δ 190.8, 152.0, 145.9, 129.8, 128.2, 115.2, 110.5, 68.2, 50.1.

Step 2 – Protection with MOMCl: To a solution of 3-(2-azidoethoxy)-4-hydroxybenzaldehyde (1.45 g, 7.00 mmol) in anhydrous acetone (6 mL), was added K₂CO₃ (1.93 g, 14.0 mmol) and methoxymethyl chloride (797 μL, 10.5 mmol). The mixture was allowed to stir at rt overnight. After removal of the solvent, water was added and the mixture was extracted 3 times with EtOAc. The combined organic layers were washed with brine, dried over anhydrous Na₂SO₄, filtered and concentrated to obtain the desired compound as a white powder (1.67 g, 6.65 mmol, **95%**). ¹H NMR (400 MHz, CDCl₃) δ 9.82 (s, 1H), 7.43 (dd, *J* = 8.2 Hz, 2.0 Hz, 1H), 7.40 (d, *J* = 1.8 Hz, 1H), 7.22 (d, *J* = 1.8 Hz, 1H), 5.26 (s, 2H), 4.23 (t, *J* = 4.9 Hz, 2H), 3.62 (t, *J* = 4.9 Hz, 2H), 3.48 (s, 3H); ¹³C NMR (100 MHz, CDCl₃) δ 190.8, 152.5, 149.0, 131.0, 127.0, 115.4, 111.6, 94.9, 68.1, 56.6, 50.1.

(E)-3-(3-(2-Azidoethoxy)-4-(methoxymethoxy)phenyl)-1-(4-chlorophenyl)prop-2-en-1-one (42). To a solution of 3-(2-azidoethoxy)-4-(methoxymethoxy)benzaldehyde **39** (0.126 g, 0.50 mmol), was added 1-(4-chlorophenyl)propan-1-one (72 μ L, 0.55 mmol) and barium hydroxide monohydrate (189 mg, 1.00 mmol). After 4 h, the mixture was concentrated under vacuum. Water was added and the aqueous layer was extracted 3 times with CH_2Cl_2 . The combined organic layers were washed with brine, dried over anhydrous Na_2SO_4 , filtered and concentrated to obtain the desired compound as a yellow powder (109 mg, 0.28 mmol, **56%**). **^1H NMR** (400 MHz, CDCl_3) δ 7.67 (d, J = 8.6 Hz, 2H), 7.41 (d, J = 15.5 Hz, 1H), 7.18 (d, J = 8.6 Hz, 2H), 7.15 (d, J = 15.5 Hz, 1H), 7.00 (d, J = 1.9 Hz, 1H), 6.97 (dd, J = 8.4, 1.9 Hz, 1H), 6.85 (d, J = 8.4 Hz, 1H), 4.94 (s, 2H), 3.96 (t, J = 4.9 Hz, 2H), 3.34 (t, J = 4.9 Hz, 2H), 3.19 (s, 3H); **^{13}C NMR** (100 MHz, CDCl_3) δ 190.7, 150.3, 149.6, 146.2, 146.1, 130.6, 129.5, 124.6, 120.8, 117.3, 114.6, 95.8, 76.3, 69.2, 56.8, 50.9, 50.1.

(E)-3-(3-(2-Aminoethoxy)-4-hydroxyphenyl)-1-(4-chlorophenyl)prop-2-en-1-one hydrochloride (45).

Step 1 - Deprotection according to general procedure C, using (E)-3-(3-(2-azidoethoxy)-4-(methoxymethoxy)phenyl)-1-(4-chlorophenyl)prop-2-en-1-one **42** (162 mg, 0.42 mmol). Yield of (E)-3-(3-(2-azidoethoxy)-4-hydroxyphenyl)-1-(4-chlorophenyl)prop-2-en-1-one was quantitative (162 mg, 0.42 mmol). **^1H NMR** (400 MHz, $\text{MeOD-}d_4$) δ 8.08 (d, J = 8.5 Hz, 2H), 7.76 (d, J = 15.6 Hz, 1H), 7.61 (d, J = 15.6 Hz, 1H), 7.56 (d, J = 8.5 Hz, 2H), 7.44 (d, J = 2.0 Hz, 1H), 7.35 (dd, J = 8.3, 2.0 Hz, 1H), 6.94 (d, J = 8.3 Hz, 1H), 4.35 (t, J = 4.9 Hz, 2H), 3.42 (t, J = 4.9 Hz, 2H); **^{13}C NMR** (100 MHz, CDCl_3) δ 191.1, 151.1, 147.8, 147.1, 140.4, 138.3, 131.4, 130.2, 128.8, 126.0, 120.3, 117.3, 114.8, 66.6, 40.6; **MS**: m/z 344.1 $[\text{M}+\text{H}]^+$.

1
2
3 Step 2 - To a solution of (*E*)-3-(3-(2-azidoethoxy)-4-hydroxyphenyl)-1-(4-chlorophenyl)prop-2-en-1-
4 one (10.0 mg, 0.03 mmol) in distilled water (0.77 mL) and THF (1.18 mL) was added polymer-
5 supported triphenylphosphine (29 mg, 0.04 mmol). The mixture was allowed to stir overnight at rt. The
6 reaction was then filtered, evaporated, purified on semi-preparative HPLC (5-70% MeCN in water),
7 treated with an aqueous solution of HCl 1M and freeze-dried to afford the title compound (5 mg, 0.02
8 mmol, **55%**) as a yellow powder. ¹H NMR (400 MHz, MeOD-*d*₄) δ 8.08 (d, *J* = 8.6 Hz, 2H), 7.76 (d, *J* =
9 15.5 Hz, 1H), 7.61 (d, *J* = 15.5 Hz, 1H), 7.56 (d, *J* = 8.5 Hz, 2H), 7.44 (d, *J* = 2.0 Hz, 1H), 7.35 (dd, *J* =
10 8.4 Hz, *J* = 2.0 Hz, 1H), 6.94 (d, *J* = 8.3 Hz, 1H), 4.35 (t, *J* = 4.9 Hz, 2H), 3.43 (t, *J* = 4.9 Hz, 2H); ¹³C
11 NMR (100 MHz, MeOD-*d*₄) δ 191.1, 151.1, 147.8, 147.1, 140.4, 138.2 (2C), 131.4, 130.2, 128.7, 126.0,
12 120.3, 117.3 (2C), 114.9, 66.6, 40.6; HRMS (ESI-TOF): calcd for C₁₇H₁₇ClNO₃ [M+H]⁺: 318.08915,
13 found: 318.08971; mp 260-262 °C; IR (Neat) 3346, 3017, 1630, 1591, 1519, 1484, 1440, 1277, 1160,
14 1015, 975, 813, 614 cm⁻¹; HPLC *t*_R = 3.90 min, purity > 98% (254 nm).

15
16
17
18
19
20
21
22
23
24
25
26
27
28
29
30
31
32
33 **4-(3-(4-Chlorophenyl)-4,5-dihydro-1H-pyrazol-5-yl)-2-methoxyphenol (50)**. To a solution of (*E*)-1-
34 (4-chlorophenyl)-3-(4-hydroxy-3-methoxyphenyl)prop-2-en-1-one **1** (524 mg, 1.81 mmol, 1 equiv) in
35 EtOH (2.6 mL) was added hydrazine monohydrate (265 μL, 5.44 mmol). The reaction was allowed to
36 reflux for 4 h. The mixture was then evaporated under reduced pressure and solubilized in EtOH (2.5
37 mL). Precipitation from *n*-heptane, centrifugation and drying *in vacuo* afforded the desired compound as
38 a white powder (457 mg, 1.51 mmol, **83%**). ¹H NMR (400 MHz, MeOD-*d*₄) δ 8.84 (br s, 1H), 7.64-7.59
39 (m, 2H), 7.57 (d, *J* = 3.2 Hz, 1H), 7.45-7.39 (m, 2H), 6.95 (d, *J* = 1.5 Hz, 1H), 6.79-6.70 (m, 2H), 4.76
40 (td, *J* = 10.9, 3.2 Hz, 1H), 3.75 (s, 3H), 3.42-3.29 (m, 1H), 2.82 (dd, *J* = 16.3 Hz, 11.0 Hz, 1H); ¹³C
41 NMR (100 MHz, MeOD-*d*₄) δ 147.5, 147.4, 145.7 (2C), 133.4, 132.3, 132.2, 128.4, 126.9, 118.9, 115.2
42 (2C), 110.8, 63.8, 55.5, 42.3; HRMS (ESI-TOF): calcd for C₁₆H₁₆ClN₂O₂ [M+H]⁺: 303.09003, found:
43
44
45
46
47
48
49
50
51
52
53
54
55

303.08959; **mp** 128-130 °C; **IR** (Neat) 3358, 1582, 1518, 1336, 1269, 1234, 1206, 1029, 827, 813, 528 cm^{-1} ; **HPLC** t_R = 3.86 min, purity > 97% (254 nm).

4-(4-Chlorophenyl)-6-(4-hydroxy-3-methoxyphenyl)pyrimidin-2(1H)-one (57). To a solution of (*E*)-1-(4-chlorophenyl)-3-(4-hydroxy-3-methoxyphenyl)prop-2-en-1-one **1** (100 mg, 0.34 mmol, 1 equiv) in EtOH (1.240 mL) was added urea (204 mg, 3.40 mmol, 10 equiv) and HCl in dioxane (840 μL , 4M). The mixture was allowed to reflux for 2 h. The reaction was then concentrated and the residue was purified on a silica gel column eluting with 0-10% MeOH in CH_2Cl_2 to afford after freeze-drying an orange powder (48 mg, 0.15 mmol, **43%**). **^1H NMR** (400 MHz, $\text{DMSO}-d_6$) δ 11.41 (br s, 1H), 10.24 (br s, 1H), 8.18 (d, J = 8.7 Hz, 2H), 7.78-7.69 (m, 2H), 7.64 (d, J = 8.7 Hz, 2H), 7.51 (s, 1H), 6.99 (d, J = 8.2 Hz, 1H), 3.90 (s, 3H); **^{13}C NMR** (100 MHz, $\text{DMSO}-d_6$) δ 163.7, 163.1, 156.6, 151.6, 147.9 (2C), 136.9, 132.6, 129.8, 128.9, 122.9, 122.6, 115.7 (2C), 111.5, 99.2, 55.9; **HRMS** (ESI-TOF): calcd for $\text{C}_{17}\text{H}_{14}\text{ClN}_2\text{O}_3$ $[\text{M}+\text{H}]^+$: 329.06875, found: 329.06876; **mp** 306-308 °C; **IR** (Neat) 3464, 1728, 1666, 1590, 1310, 1262, 1216, 1153, 1089, 795, 774, 622, 490 cm^{-1} . **HPLC** t_R = 3.46 min, purity > 97% (254 nm).

(E)-7-Chloro-3-(4-hydroxy-3-methoxybenzylidene)chroman-4-one (65). To a solution 7-chlorochroman-4-one (156 mg, 0.86 mmol) and 4-hydroxy-3-methoxybenzaldehyde (131 mg, 0.86 mmol) in EtOH (1.80 mL), SOCl_2 (88 μL , 1.00 mmol) was added dropwise at rt. The reaction mixture was stirred for 5 h. The solvent was then evaporated *in vacuo* and the crude product was recrystallized from EtOH affording the desired compound (145 mg, 0.46 mmol, **53%**) as a yellow solid. **^1H NMR** (400 MHz, CDCl_3) δ 7.93 (d, J = 8.5 Hz, 1H), 7.79 (t, J = 1.9 Hz, 1H), 7.02 (dd, J = 8.5, 2.0 Hz, 1H), 6.98 (d, J = 7.8 Hz, 1H), 6.97 (d, J = 2.0 Hz, 1H), 6.82 (d, J = 2.0 Hz, 1H), 6.81 (dd,

1
2
3 $J = 7.8, 2.0$ Hz, 1H), 5.92 (s, 1H), 5.37 (d, $J = 1.9$ Hz, 2H), 3.91 (s, 3H); ^{13}C NMR (100 MHz, CDCl_3) δ
4 181.4, 161.5, 147.7, 146.8, 141.7, 138.5, 129.3, 128.4, 126.9, 124.5, 122.8, 120.8, 118.2, 115.0, 113.1,
5 68.4, 56.2; HRMS (ESI-TOF): calcd for $\text{C}_{17}\text{H}_{14}\text{ClO}_4$ $[\text{M}+\text{H}]^+$: 317.0575, found: 317.0583; mp 180-
6 182 °C; IR (Neat) 3502, 1658, 1567, 1512, 1444, 1261, 1206, 1127, 1027, 842, 805, 490 cm^{-1} ; HPLC t_R
7 = 5.70 min, purity > 97% (254 nm).
8
9
10
11
12
13
14
15
16

17 **(E)-1-(4-Chloro-2-hydroxyphenyl)-3-(3-methoxy-4-(methoxymethoxy)phenyl)prop-2-en-1-one**

18
19 **(66)**. To a solution of 3-(2-azidoethoxy)-4-(methoxymethoxy)benzaldehyde (180 mg, 0.92 mmol) in
20 EtOH (2.5 mL), was added 1-(4-chloro-2-hydroxyphenyl)ethan-1-one (234 mg, 1.34 mmol) and
21 $\text{Ba}(\text{OH})_2 \cdot \text{H}_2\text{O}$ (157 mg, 0.83 mmol). The reaction was stirred for 48 h at rt. The mixture was evaporated.
22 Purification on flash chromatography eluting with 5-100% EtOAc in *n*-heptane afford the desired
23 product (100 mg, 0.29 mmol, **28%**). The corresponding product was directly engaged in the next step
24 without analysis.
25
26
27
28
29
30
31
32
33
34

35 **(Z)-6-Chloro-2-(4-hydroxy-3-methoxybenzylidene)benzofuran-3(2H)-one (67)**. (E)-1-(4-chloro-2-
36 hydroxyphenyl)-3-(3-methoxy-4-(methoxymethoxy)phenyl)prop-2-en-1-one **66** (40 mg, 0.11 mmol, see
37 SI) was added to 0.1 M $\text{Hg}(\text{AcO})_2$ in anhydrous pyridine (1.14 mL). The mixture was stirred for 1 h at
38 110 °C. After cooling, it was poured into ice/water (100 mL) and acidified with a 1 M aqueous HCl. The
39 precipitate was recovered, dissolved with CH_2Cl_2 (5 mL) and washed once with water, then with brine.
40 The organic layer was dried over anhydrous Na_2SO_4 and the solvent was evaporated *in vacuo*. The crude
41 was purified by flash chromatography on a silica gel column eluting with 10-50% EtOAc in *n*-heptane
42 affording 12 mg (0.029 mmol, **25%**) of protected compound. The title compound was obtained after
43 deprotection according to general procedure C (quantitative yield). ^1H NMR (400 MHz, CDCl_3) δ 9.92
44
45
46
47
48
49
50
51
52
53
54
55

(br s, 1H), 7.86-7.76 (m, 2H), 7.62 (s, 1H), 7.51 (br d, $J = 8.2$ Hz, 1H), 7.36 (br d, $J = 8.1$ Hz, 1H), 6.95 (s, 1H), 6.91 (br d, $J = 8.2$ Hz, 1H), 3.86 (s, 3H); ^{13}C NMR (100 MHz, CDCl_3) δ 181.7, 165.1, 149.7, 147.8, 144.9, 141.1, 126.3, 125.3, 124.2, 122.9, 120.3, 116.0, 115.2, 114.5, 113.8, 55.6; HRMS (ESI-TOF): calcd for $\text{C}_{16}\text{H}_{12}\text{ClO}_4$ $[\text{M}+\text{H}]^+$: 303.04241, found: 303.04182; mp 206-208 °C; IR (Neat) 3545, 1696, 1646, 1600, 1582, 1518, 1307, 1267, 1201, 1137, 1125, 1057, 1032, 841, 764 cm^{-1} ; HPLC $t_R = 5.42$ min, purity > 98% (254 nm).

Physicochemical properties

Solubility and stability studies were performed using a Gilson HPLC system with a photodiode array detector for the analyses. Data acquisition and processing were performed with Trilution LC V2.0 software. Measurements were carried out at room temperature. A 5 μm Luna C18(2) (50 X 4.6 mm) purchased from Phenomenex was used. The mobile phase flow rate was 2 mL/min and the following program was applied for the elution: 0-0.7 min, 0% B; 0.7-3.2 min, 0-100% B; 3.2-3.7 min, 100% B; 3.7-3.9 min, 100-0% B and 3.9-6.7 min, 0% B. Solvent B was HPLC grade acetonitrile (Sigma-Aldrich CHROMASOLV). The aqueous solvent contained 0.01 % trifluoroacetic acid. The detection wavelengths were 280 and 365 nm.

Solubility. Kinetic solubility was measured for all the compounds in a pH 7.4 HEPES-BSA buffer with the following composition: NaCl 137.5 mM, MgCl_2 1.25 mM, CaCl_2 1.25 mM, KCl 6 mM, glucose 5.6 mM, NaH_2PO_4 0.4 mM, HEPES 10 mM and 1 g/L bovine serum albumin. This method mimicked the conditions of the FRET-based binding experiments. Every compound was initially pre-dissolved in DMSO at 10 mM. An aliquot of the DMSO solution was added to the buffer to reach a 5 μM

1
2
3 concentration. Samples were shaken during 24 hours at 20 °C. After centrifugation, the concentration in
4
5 the supernatant was measured by a HPLC procedure using two standard solutions (5 and 10 μM).

6
7
8 Thermodynamic solubility was measured for seven selected compounds by dissolving powders until
9
10 saturation in pH 7.4 PBS (phosphate-buffered saline containing 100 mM sodium phosphate and 150 mM
11
12 sodium chloride). Samples were shaken during 24 hours at 20 °C. After centrifugation, the concentration
13
14 in the supernatant was measured by a HPLC procedure using a calibration line established for each
15
16 compound by diluting the 10 mM DMSO stock solution to adapted concentrations.
17
18
19
20

21 **Chemical stability.** Stability of the same seven compounds selected for the thermodynamic solubility
22
23 study was assessed in PBS pH 7.4 or PBS/Cdx (10% w/w) at 20°C for up to 24 hours. For each
24
25 compound, the stock solution was diluted to a final incubation concentration of 10 μM with 1% DMSO.
26
27 50 μL of sample were removed at t_0 , 2, 4, 6 and 24 hours and directly injected onto the HPLC. The
28
29 percentage of remaining test compound relative to t_0 was measured by monitoring the peak area of the
30
31 chromatogram.
32
33
34
35
36
37

38 **Michael addition.** Michael acceptor reactivity was evaluated by incubating the compounds with
39
40 reduced glutathione (GSH). Incubation mixtures contained: 250 μL methanol, 500 μM GSH (25 μL of a
41
42 10 mM GSH solution), 200 μM compound (10 μL of the 10 mM DMSO stock solution) and 215 μL of a
43
44 50 mM carbonate buffer adjusted at pH 8 (final volume of 500 μL). Five μL-aliquots of the reaction
45
46 mixture were removed after 1 min and 2 hours incubation. Samples were diluted 1/40 in water 0.05%
47
48 formic acid/acetonitrile 1/1 and analyzed by LC-MS/MS for GSH-conjugate formation.
49
50
51
52
53
54
55
56
57
58
59
60

1
2
3 **Computational methods.** Starting from the X-ray structure of the CXCL12 bound to inhibitor 3GG
4 (PDB ID 4UAI), all non-protein atoms (inhibitor, sulfate ions, water molecules) were removed and
5
6 hydrogens added with Protoss v2.1⁴¹ while optimizing protonation, ionization and tautomeric states of
7
8 all protein atoms. A 2D sketch of compound **1** was converted into a 2D MOL2 file with Corina v3.40
9
10 (Molecular Networks GmbH, Erlangen, Germany). The crystal structure of compound **57** (Figure S1)
11
12 was converted into a MOL2 file format and used as such for docking with PLANTS v.1.2.³⁶ The binding
13
14 site was defined as 12 Å-radius sphere centered on the center of mass of the Trp57 cavity, deduced from
15
16 the VolSite software.³⁵ Three side chains (Arg20, Trp57 and Tyr61) were allowed to freely move during
17
18 the docking, performed with the speed1 search speed and the chemplp scoring function. For Surflex-
19
20 Dock v3.066³⁷ a "protomol" was first generated using a list of binding site residues encompassing the
21
22 above-described 12 Å sphere. The protein residues side-chains were kept rigid, excepted for Arg20,
23
24 Trp57 and Tyr61 which were considered fully flexible. Other parameters were assigned as default. The
25
26 docking accuracy parameter set -pgeom was used.
27
28
29
30
31
32
33

34 **Biological evaluation**

35
36 **Generation of HEK-293 cells stably expressing human CXCR4 chemokine receptor.** Human cDNA
37
38 encoding CXCR4 receptor was cloned in pCEP4 vector (Life technologies). The receptor is cloned in
39
40 frame with a signal peptide fused to enhanced green fluorescent protein (EGFP) as described previously.
41
42 The open reading frame was fully sequenced prior to transfection. Human Embryonic Kidney HEK-293
43
44 cells were obtained from ATCC and maintained in minimal essential medium (MEM) (Invitrogen)
45
46 supplemented with 10% fetal bovine serum (FBS) (Gibco-BRL), 100 U/ml penicillin (Invitrogen), 100
47
48 µg/ml streptomycin (Invitrogen) and 2 mM L-glutamine (Invitrogen) at 37 °C in an atmosphere of 95%
49
50 air and 5% CO₂. HEK-293 cells were transfected with 15 µg of the human CXCR4 chemokine receptor
51
52
53
54
55
56
57
58
59
60

1
2
3 in pCEP4 plasmid using a calcium phosphate precipitation method in 10 cm dishes. Stably EGFP-
4 CXCR4-expressing HEK cells were selected by addition of hygromycin (Life technologies) for 5 weeks.
5
6 The resulting cell clones were checked by fluorescence microscopy and fluorescence-activated cell
7
8 sorting (FACS) analysis.
9
10

11
12
13
14 **FRET-based binding assay.** HEK EGFP-CXCR4 expressing cells were washed with phosphate
15 buffered saline (PBS) and detached in PBS-ethylene diamine tetra-acetic acid (EDTA, 5 mM) (Sigma-
16 Aldrich) for 2 min at room temperature. Then, cells were carefully resuspended in complete growth
17 medium, pelleted by centrifugation at 320×g for 5 min, and resuspended in HEPES buffer (137.5 mM
18 NaCl, 6 mM KCl, 1.25 mM CaCl₂, 1.25 mM MgCl₂, 0.4 mM NaH₂PO₄, 5.6 mM glucose, 10 mM
19 HEPES (4-(2-hydroxyethyl)-1-piperazineethanesulfonic acid), pH 7.4) containing 0.1% bovine serum
20 albumin (w/v) (BSA) (all from Sigma-Aldrich). Cells were used at a concentration of 10⁶ cells/ml,³⁴
21 then the cell suspension (1 ml) was transferred into a quartz cuvette. Time-based recordings of the
22 fluorescence emitted at 510 nm (excitation at 470 nm) were performed at 21 °C using a Fluorolog 3
23 spectrofluorometer (JobinYvon/Spex). Fluorescence binding measurements were initiated by adding at
24 t=150 s, 100 nM CXCL12-Texas Red (TR) (Almac) to the 1-ml cell suspension. Binding of CXCL12-
25 TR to EGFP-labeled CXCR4 was detected as a reversible decline of emission at 510 nm, due to energy
26 transfer from excited EGFP to TR. In the “neutraligand protocol”, CXCL12-TR was preincubated for 1h
27 at room temperature with DMSO or various concentrations of each test compound. Then the premix was
28 added (at t=150 s), and fluorescence was recorded until equilibrium was reached (300 s). In the
29 “antagonist protocol”, DMSO or various concentrations of each test compound were added to EGFP-
30 CXCR4-expressing cells at t=50 s. Then CXCL12-Texas Red (100 nM) was added at t=150 s, and
31 fluorescence was recorded until equilibrium was reached (300 sec). Dose-response curves of inhibition
32
33
34
35
36
37
38
39
40
41
42
43
44
45
46
47
48
49
50
51
52
53
54
55

1
2
3 of CXCL12-TR binding were performed and the inhibitory constants (K_i) of the different compounds
4
5 were determined. T134 (20 μ M), the CXCR4 receptor antagonist, was used as a control in both
6
7 “neutraligand” and “antagonist” protocols. Data were analysed using Kaleidagraph 4.1.3 software
8
9 (Synergy Software, Reading, PA).
10
11
12
13

14
15 **Allergic eosinophilic airway inflammation mouse model.** The activity of each compound was
16
17 assessed *in vivo* in an 8 day model of allergic eosinophilic airway inflammation as described
18
19 previously.^{21, 33} Briefly, 9 week-old male Balb/c mice were sensitized by intraperitoneal injection of 50
20
21 μ g of ovalbumin (OVA, grade V, Sigma-Aldrich, A5503) adsorbed on 2 mg of aluminium hydroxide
22
23 (Sigma-Aldrich, 23918-6) in 0.1 mL of saline on days 0, 1, and 2. Mice were challenged intranasally [10
24
25 μ g of OVA in 25 μ L of saline (12.5 μ L/nostril)] on days 5, 6, and 7. Control mice received intranasal
26
27 administration of saline alone. Intranasal administrations were performed under anaesthesia with
28
29 intraperitoneal injection of ketamine (50 mg/kg) and xylazine (3.33 mg/kg). Food and water were
30
31 supplied *ad libitum*. Animal experimentation was conducted with the approval of the agriculture
32
33 ministry regulating animal research in France (Ethics regional committee for animal experimentation-
34
35 Strasbourg, APAFIS 1341#2015080309399690). Two hours before each OVA or saline challenge,
36
37 compounds in PBS/Cdx were administered intranasally (12.5 μ L/nostril), intraperitoneally or *per os* as
38
39 indicated in the figure legends. Bronchoalveolar lavage (BAL) was performed 24 hours after the last
40
41 OVA or saline challenge as described.³⁴ Mice were deeply anesthetized by intraperitoneal injection of
42
43 ketamine (Imalgene[®], 150 mg/kg) and xylazine (Rompun[®], 10 mg/kg). A plastic cannula was inserted
44
45 into the trachea, and airways were lavaged by 10 instillations of 0.5 mL of ice-cold saline supplemented
46
47 with 2.6 mM EDTA (saline-EDTA). BAL fluids were centrifuged (300g, 5 min, 4 °C) to pellet cells, and
48
49 erythrocytes were lysed by hypotonic shock. Cells were resuspended in 500 μ L of ice-cold saline-
50
51
52
53
54
55
56
57
58
59
60

1
2
3 EDTA, and total cell counts were determined on a hemocytometer (Neubauer, PRECISS[®]). Differential
4
5 cell counts were assessed on cytological preparations (Cytospin 4, Thermo Fischer Scientific) spanning
6
7 250 000 cells/mL in ice-cold saline-EDTA, stained with Diff-Quick[®] (Merck, 111674) with counts of at
8
9 least 400 cells. Counts were expressed as absolute cell numbers or percentage of inhibition of eosinophil
10
11 recruitment. The differential number of cells in BALF and the eosinophil inhibition (%) are presented as
12
13 means \pm SEM. Differences between groups were tested for statistical significance using a one-way
14
15 ANOVA followed by Tukey post-test. Data were considered significantly different when p value <0.05 .
16
17
18
19
20
21
22
23
24
25
26
27
28
29
30
31
32
33
34
35
36
37
38
39
40
41
42
43
44
45
46
47
48
49
50
51
52
53
54
55
56
57
58
59
60

ANCILLARY INFORMATION

Supporting information: General procedures and experimental data for compounds **2-21**, **23-28**, **30-38**, **40**, **41**, **43**, **44**, **46-49**, **51-56**, **58-64** and **68**; crystallographic structure for **1** and **57** (CCDC 1578824-1578825, Figure S1, Tables S1 and S2) and chemical stability study of **1** and **57** toward reduced glutathione (Figure S2); molecular formula strings This material is available free of charge via the Internet at <http://pubs.acs.org>

Corresponding Author Information: Dr Nelly Frossard; Email: nelly.frossard@unistra.fr; Dr Dominique Bonnet; Email: dominique.bonnet@unistra.fr.

Acknowledgments: This work was supported by the Agence Nationale de la Recherche (ANR-07-PCVI-0026-02), the Centre National de la Recherche Scientifique, the Université de Strasbourg and the LABEX Medalis (ANR-10-LABX-0034). PR was supported by a fellowship from the Ministère de l'Éducation Nationale, de l'Enseignement Supérieur et de la Recherche. FD was recipient of fellowships from the Fonds de recherche en santé respiratoire (FRSR) and Région Alsace. DA was a fellow of the CNRS and of Greenpharma SA. We are grateful to Cyril Antheaume, Barbara Schaeffer and Justine Vieville for NMR experiments, to Pascale Buisine and Patrick Wehrung for mass spectrometry (PACSI platform GDS3670) and to Lydia Karmazin for crystallographic structures (Service de Radiocristallographie, Platform GDS 3648, Strasbourg).

Abbreviations: BAL, bronchoalveolar lavage; BSA, bovine serum albumin; Cdx, 2-hydroxypropyl- β -cyclodextrin; CXCL12, C-X-C chemokine 12; CXCR4, C-X-C chemokine receptor type 4; G6P, glucose-6-phosphate; G6PDH, glucose-6-phosphate dehydrogenase; HEPES, 4-(2-hydroxyethyl)-1-

1
2
3 piperazineethanesulfonic acid; HIV, human immunodeficiency virus; in, intranasal ; LC-MS, liquid
4 chromatography-mass spectrometry; MOM, methoxymethyl; NADP, nicotinamide adenine dinucleotide
5 phosphate; OVA, ovalbumin; PBS, phosphate-buffered saline; PS, polymer-supported; RP-HPLC,
6 reversed-phase high-performance liquid chromatography; SAR, structure-activity relationship; SEM,
7 standard error of the mean; TBDMS, *tert*-butyldimethylsilyl; TCEP, tris (2-carboxyethyl) phosphine;
8 TR, Texas-red; WHIM, warts, hypogammaglobulinemia, infections, and myelokathexis.
9
10
11
12
13
14
15
16
17
18
19
20
21
22
23
24
25
26
27
28
29
30
31
32
33
34
35
36
37
38
39
40
41
42
43
44
45
46
47
48
49
50
51
52
53
54
55
56
57
58
59
60

REFERENCES

1. Zou, Y.-R.; Kottmann, A. H.; Kuroda, M.; Taniuchi, I.; Littman, D. R. Function of the chemokine receptor CXCR4 in haematopoiesis and in cerebellar development. *Nature* **1998**, *393*, 595-599.
2. Tran, P. B.; Miller, R. J. Chemokine receptors: signposts to brain development and disease. *Nat. Rev. Neurosci.* **2003**, *4*, 444-455.
3. Fernandez, E. J.; Lolis, E. Structure, function, and inhibition of chemokines. *Annu. Rev. of Pharmacol. Toxicol.* **2002**, *42*, 469-499.
4. Mantovani, A. The chemokine system: redundancy for robust outputs. *Immunol. Today* **1999**, *20*, 254-257.
5. Johnson, Z.; Schwarz, M.; Power, C. A.; Wells, T. N. C.; Proudfoot, A. E. I. Multi-faceted strategies to combat disease by interference with the chemokine system. *Trends Immunol.* **2005**, *26*, 268-274.
6. Moser, B.; Willmann, K. Chemokines: role in inflammation and immune surveillance. *Ann. Rheum. Dis.* **2004**, *63*, 84-89.
7. Godessart, N.; Kunkel, S. L. Chemokines in autoimmune disease. *Curr. Opin. Immunol.* **2001**, *13*, 670-675.
8. Lazenec, G.; Richmond, A. Chemokines and chemokine receptors: new insights into cancer-related inflammation. *Trends Mol. Med.* **2010**, *16*, 133-144.
9. Balkwill, F. R. The chemokine system and cancer. *J. Pathol.* **2012**, *226*, 148-157.
10. Koenen, R. R.; Weber, C. Therapeutic targeting of chemokine interactions in atherosclerosis. *Nat. Rev. Drug Discov.* **2010**, *9*, 141-153.

- 1
2
3 11. Braunersreuther, V.; Mach, F.; Steffens, S. The specific role of chemokines in atherosclerosis.
4
5 *Thromb. Haemost.* **2007**, *97*, 714-721.
6
7
8 12. Wenzel, J.; Henze, S.; Worenkamper, E.; Basner-Tschakarjan, E.; Sokolowska-Wojdylo, M.;
9
10 Steitz, J.; Bieber, T.; Tuting, T. Role of the chemokine receptor CCR4 and its ligand thymus- and
11
12 activation-regulated chemokine/CCL17 for lymphocyte recruitment in cutaneous lupus erythematosus.
13
14 *J. Invest. Dermatol.* **2005**, *124*, 1241-1248.
15
16
17 13. Bendall, L. Chemokines and their receptors in disease. *Histol. Histopathol.* **2005**, *20*, 907-926.
18
19
20 14. Zipp, F.; Hartung, H. P.; Hillert, J.; Schimrigk, S.; Trebst, C.; Stangel, M.; Infante-Duarte, C.;
21
22 Jakobs, P.; Wolf, C.; Sandbrink, R.; Pohl, C.; Filippi, M. Blockade of chemokine signaling in patients
23
24 with multiple sclerosis. *Neurology* **2006**, *67*, 1880-1883.
25
26
27 15. Brown, M. F.; Bahnck, K. B.; Blumberg, L. C.; Brissette, W. H.; Burrell, S. A.; Driscoll, J. P.;
28
29 Fedeles, F.; Fisher, M. B.; Foti, R. S.; Gladue, R. P.; Guzman-Martinez, A.; Hayward, M. M.; Lira, P.
30
31 D.; Lillie, B. M.; Lu, Y.; Lundquist, G. D.; McElroy, E. B.; McGlynn, M. A.; Paradis, T. J.; Poss, C. S.;
32
33 Roache, J. H.; Shavnya, A.; Shepard, R. M.; Trevena, K. A.; Tylaska, L. A. Piperazinyl CCR1
34
35 antagonists--optimization of human liver microsome stability. *Bioorg. Med. Chem. Lett.* **2007**, *17*, 3109-
36
37 3112.
38
39
40 16. Johnson, M.; Li, A. R.; Liu, J.; Fu, Z.; Zhu, L.; Miao, S.; Wang, X.; Xu, Q.; Huang, A.; Marcus,
41
42 A.; Xu, F.; Ebsworth, K.; Sablan, E.; Danao, J.; Kumer, J.; Dairaghi, D.; Lawrence, C.; Sullivan, T.;
43
44 Tonn, G.; Schall, T.; Collins, T.; Medina, J. Discovery and optimization of a series of quinazolinone-
45
46 derived antagonists of CXCR3. *Bioorg. Med. Chem. Lett.* **2007**, *17*, 3339-3343.
47
48
49 17. Horuk, R. Chemokine receptor antagonists: overcoming developmental hurdles. *Nat. Rev. Drug*
50
51 *Discov.* **2009**, *8*, 23-33.
52
53
54
55
56
57
58
59
60

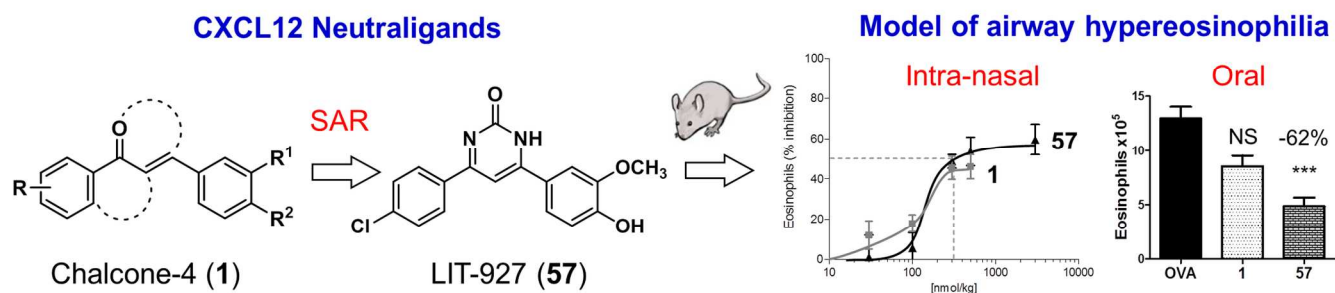
- 1
2
3 18. Hachet-Haas, M.; Balabanian, K.; Rohmer, F.; Pons, F.; Franchet, C.; Lecat, S.; Chow, K. Y.;
4
5 Dagher, R.; Gizzi, P.; Didier, B.; Lagane, B.; Kellenberger, E.; Bonnet, D.; Baleux, F.; Haiech, J.;
6
7 Parmentier, M.; Frossard, N.; Arenzana-Seisdedos, F.; Hibert, M.; Galzi, J. L. Small neutralizing
8
9 molecules to inhibit actions of the chemokine CXCL12. *J. Biol. Chem.* **2008**, *283*, 23189-23199.
- 10
11
12 19. Balabanian, K.; Brotin, E.; Biajoux, V.; Bouchet-Delbos, L.; Lainey, E.; Fenneteau, O.; Bonnet,
13
14 D.; Fiette, L.; Emilie, D.; Bachelerie, F. Proper desensitization of CXCR4 is required for lymphocyte
15
16 development and peripheral compartmentalization in mice. *Blood* **2012**, *119*, 5722-5730.
- 17
18
19 20. Romain, B.; Hachet-Haas, M.; Rohr, S.; Brigand, C.; Galzi, J. L.; Gaub, M. P.; Pencreach, E.;
20
21 Guenot, D. Hypoxia differentially regulated CXCR4 and CXCR7 signaling in colon cancer. *Mol.*
22
23 *Cancer* **2014**, 13:58.
- 24
25
26 21. Gasparik, V.; Daubeuf, F.; Hachet-Haas, M.; Rohmer, F.; Gizzi, P.; Haiech, J.; Galzi, J. L.;
27
28 Hibert, M.; Bonnet, D.; Frossard, N. Prodrugs of a CXC Chemokine-12 (CXCL12) Neutraligand prevent
29
30 inflammatory reactions in an asthma model in vivo. *ACS Med. Chem. Lett.* **2012**, *3*, 10-14.
- 31
32
33 22. Daubeuf, F.; Hachet-Haas, M.; Gizzi, P.; Gasparik, V.; Bonnet, D.; Utard, V.; Hibert, M.;
34
35 Frossard, N.; Galzi, J. L. An antedrug of the CXCL12 neutraligand blocks experimental allergic asthma
36
37 without systemic effect in mice. *J. Biol. Chem.* **2013**, *288*, 11865-11876.
- 38
39
40 23. Veldkamp, C. T.; Ziarek, J. J.; Peterson, F. C.; Chen, Y.; Volkman, B. F. Targeting SDF-
41
42 1/CXCL12 with a ligand that prevents activation of CXCR4 through structure-based drug design. *J. Am.*
43
44 *Chem. Soc.* **2010**, *132*, 7242-7243.
- 45
46
47 24. Smith, E. W.; Liu, Y.; Getschman, A. E.; Peterson, F. C.; Ziarek, J. J.; Li, R. S.; Volkman, B. F.;
48
49 Chen, Y. Structural analysis of a novel small molecule ligand bound to the CXCL12 chemokine. *J. Med.*
50
51 *Chem.* **2014**, *57*, 9693-9699.
- 52
53
54
55
56
57
58
59
60

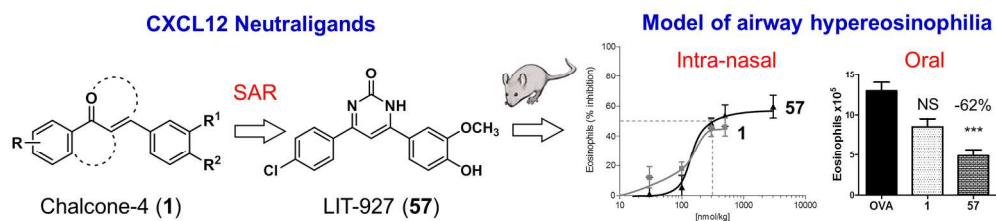
- 1
2
3 25. Smith, E. W.; Nevins, A. M.; Qiao, Z.; Liu, Y.; Getschman, A. E.; Vankayala, S. L.; Kemp, M.
4
5 T.; Peterson, F. C.; Li, R. S.; Volkman, B. F.; Chen, Y. Structure-based identification of novel ligands
6
7 targeting multiple sites within a chemokine–G-protein-coupled-receptor interface. *J. Med. Chem.* **2016**,
8
9 *59*, 4342-4351.
- 10
11
12 26. Weisberg, E. L.; Sattler, M.; Azab, A. K.; Eulberg, D.; Kruschinski, A.; Manley, P. W.; Stone,
13
14 R.; Griffin, J. D. Inhibition of SDF-1-induced migration of oncogene-driven myeloid leukemia by the L-
15
16 RNA aptamer (Spiegelmer), NOX-A12, and potentiation of tyrosine kinase inhibition. *Oncotarget* **2017**,
17
18 *8*, 109973-109984.
- 19
20
21 27. Rucker, H.; Al-Rifai, N.; Rasclé, A.; Gottfried, E.; Brodziak-Jarosz, L.; Gerhauser, C.; Dick, T.
22
23 P.; Amslinger, S. Enhancing the anti-inflammatory activity of chalcones by tuning the Michael acceptor
24
25 site. *Org. Biomol. Chem.* **2015**, *13*, 3040-3047.
- 26
27
28 28. Chimenti, F.; Fioravanti, R.; Bolasco, A.; Manna, F.; Chimenti, P.; Secci, D.; Befani, O.; Turini,
29
30 P.; Ortuso, F.; Alcaro, S. Monoamine oxidase isoform-dependent tautomeric influence in the recognition
31
32 of 3,5-diaryl pyrazole inhibitors. *J. Med. Chem.* **2007**, *50*, 425-428.
- 33
34
35 29. Maillet, E. L.; Pellegrini, N.; Valant, C.; Bucher, B.; Hibert, M.; Bourguignon, J. J.; Galzi, J. L.
36
37 A novel, conformation-specific allosteric inhibitor of the tachykinin NK2 receptor (NK2R) with
38
39 functionally selective properties. *FASEB J.* **2007**, *21*, 2124-2134.
- 40
41
42 30. Valenzuela-Fernandez, A.; Palanche, T.; Amara, A.; Magerus, A.; Altmeyer, R.; Delaunay, T.;
43
44 Virelizier, J. L.; Baleux, F.; Galzi, J. L.; Arenzana-Seisdedos, F. Optimal inhibition of X4 HIV isolates
45
46 by the CXC chemokine stromal cell-derived factor 1 alpha requires interaction with cell surface heparan
47
48 sulfate proteoglycans. *J. Biol. Chem.* **2001**, *276*, 26550-26558.
- 49
50
51 31. Galzi, J.-L.; Haas, M.; Frossard, N.; Hibert, M. Why and how to find neutraligands targeting
52
53 chemokines? *Drug Discov. Today* **2012**, *9*, 245-251.
- 54
55
56
57
58
59
60

- 1
2
3 32. Gould, S.; Scott, R. C. 2-Hydroxypropyl-beta-cyclodextrin (HP-beta-CD): a toxicology review.
4
5 *Food Chem. Toxicol.* **2005**, *43*, 1451-1459.
6
7
8 33. Daubeuf, F.; Frossard, N. Acute asthma models to ovalbumin in the mouse. In *Curr. Protoc.*
9
10 *Mouse Biol.* **2013**, *3*, 31-37.
11
12 34. Daubeuf, F.; Frossard, N. Performing bronchoalveolar lavage in the mouse. In *Curr. Protoc.*
13
14 *Mouse Biol.* **2012**, *2*, 167-175.
15
16
17 35. Desaphy, J.; Azdimousa, K.; Kellenberger, E.; Rognan, D. Comparison and druggability
18
19 prediction of protein-ligand binding sites from pharmacophore-annotated cavity shapes. *J. Chem. Inf.*
20
21 *Model.* **2012**, *52*, 2287-2299.
22
23
24 36. Korb, O.; Stutzle, T.; Exner, T. E. Empirical scoring functions for advanced protein-ligand
25
26 docking with PLANTS. *J. Chem. Inf. Model.* **2009**, *49*, 84-96.
27
28
29 37. Jain, A. N. Surflex-Dock 2.1: Robust performance from ligand energetic modeling, ring
30
31 flexibility, and knowledge-based search. *J. Comput. Aided Mol. Des.* **2007**, *21*, 281-306.
32
33
34 38. Schneider, N.; Lange, G.; Hindle, S.; Klein, R.; Rarey, M. A consistent description of HYdrogen
35
36 bond and DEhydration energies in protein-ligand complexes: methods behind the HYDE scoring
37
38 function. *J. Comput. Aided Mol. Des.* **2013**, *27*, 15-29.
39
40
41 39. Abboud, D.; Daubeuf, F.; Do, Q. T.; Utard, V.; Villa, P.; Haiech, J.; Bonnet, D.; Hibert, M.;
42
43 Bernard, P.; Galzi, J. L.; Frossard, N. A strategy to discover decoy chemokine ligands with an anti-
44
45 inflammatory activity. *Sci. Rep.* **2015**, *5*, 2045-2322.
46
47
48 40. Lukacs, N. W.; Berlin, A.; Schols, D.; Skerlj, R. T.; Bridger, G. J. AMD3100, a CxCR4
49
50 antagonist, attenuates allergic lung inflammation and airway hyperreactivity. *American Journal of*
51
52 *Pathology* **2002**, *160*, 1353-1360.
53
54
55
56
57
58
59
60

1
2
3 41. Bietz, S.; Urbaczek, S.; Schulz, B.; Rarey, M. Protoss: a holistic approach to predict tautomers
4 and protonation states in protein-ligand complexes. *J. Cheminform.* **2014**, 6:12.
5
6
7
8
9
10
11
12
13
14
15
16
17
18
19
20
21
22
23
24
25
26
27
28
29
30
31
32
33
34
35
36
37
38
39
40
41
42
43
44
45
46
47
48
49
50
51
52
53
54
55
56
57
58
59
60

Table of Contents Graphic





TOC

196x46mm (300 x 300 DPI)

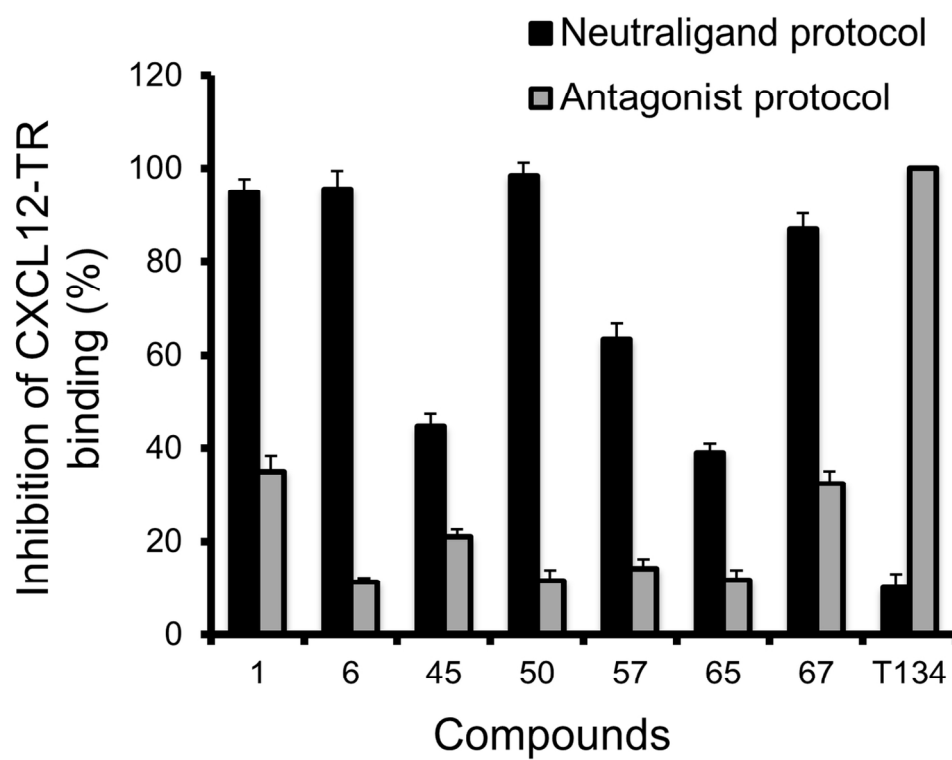


Figure 3

127x99mm (300 x 300 DPI)

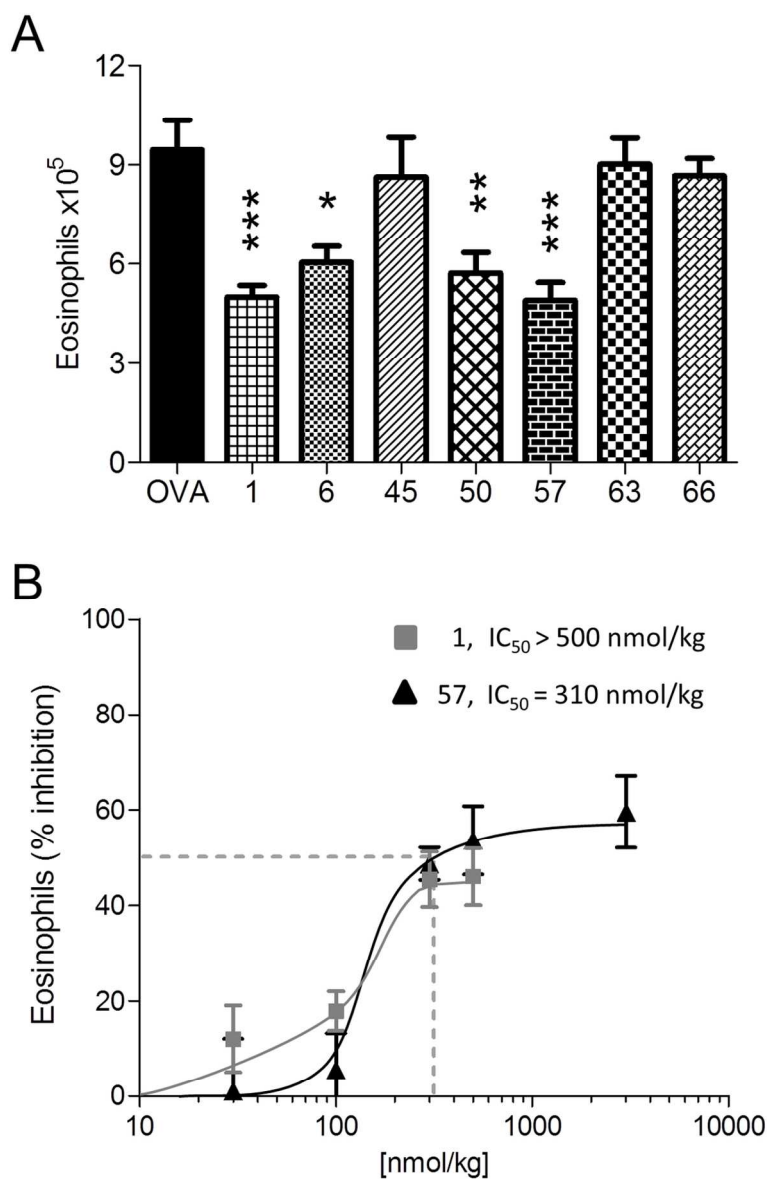


Figure 4

104x153mm (300 x 300 DPI)

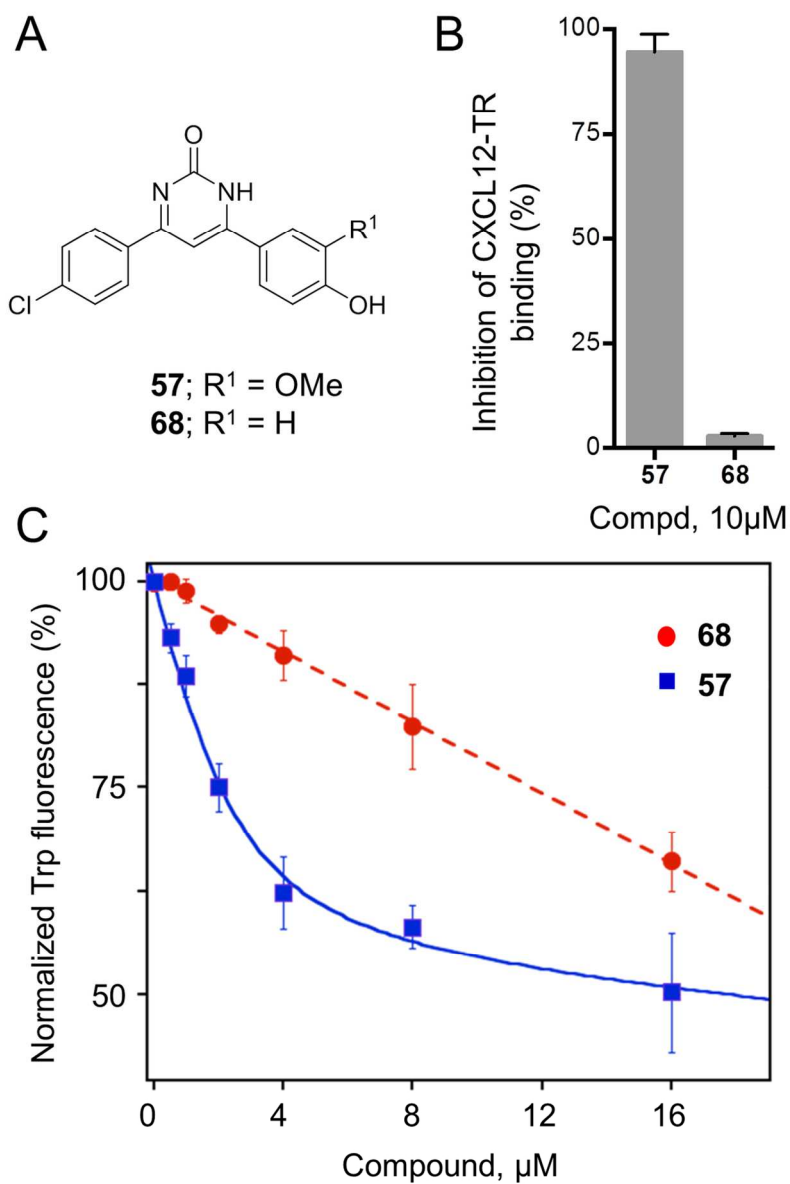


Figure 5

110x160mm (300 x 300 DPI)

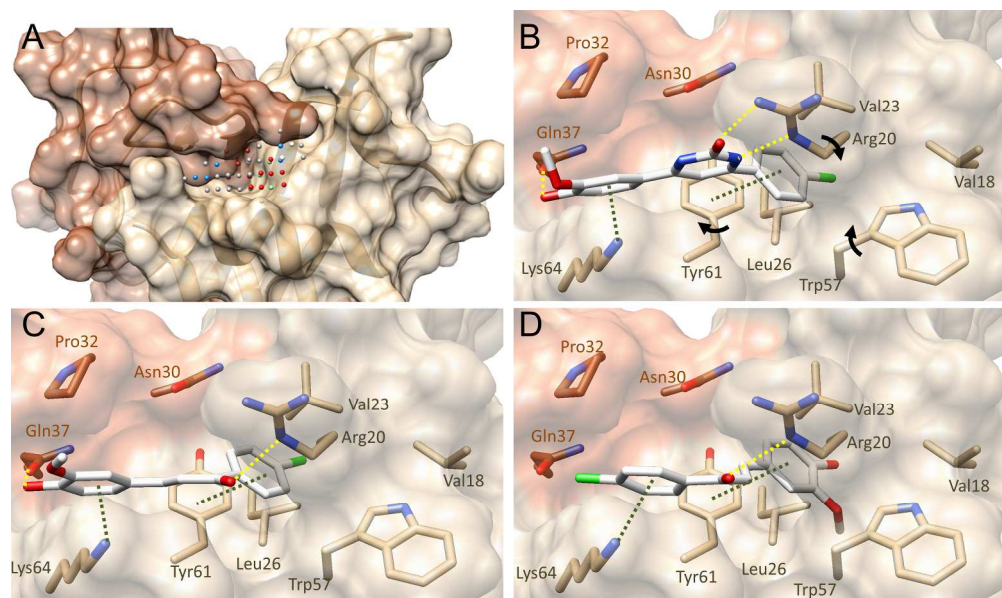


Figure 6

247x145mm (300 x 300 DPI)

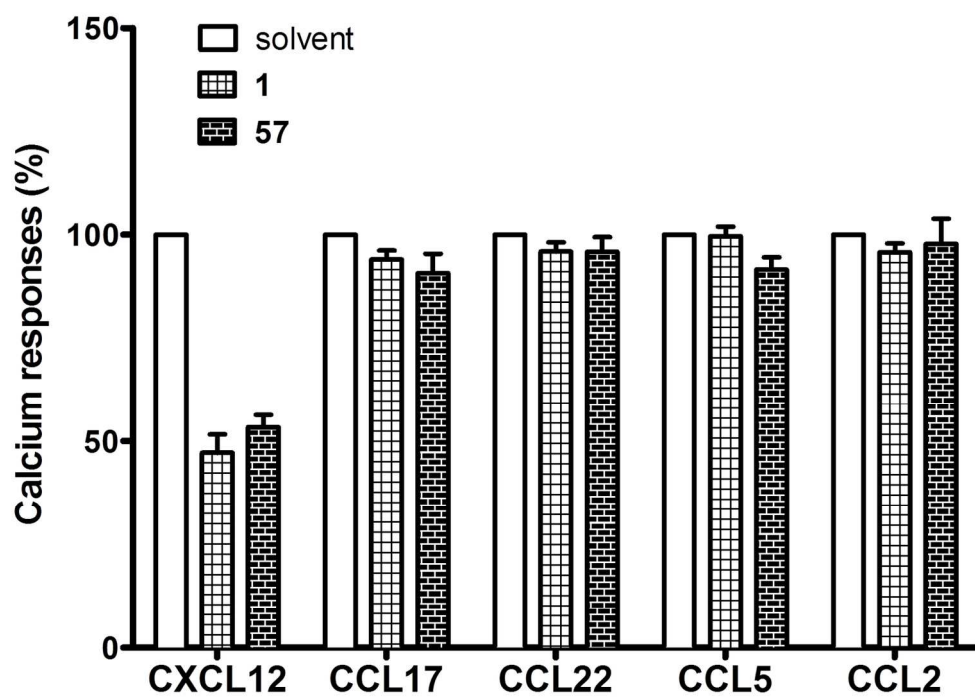


Figure 7

154x110mm (300 x 300 DPI)

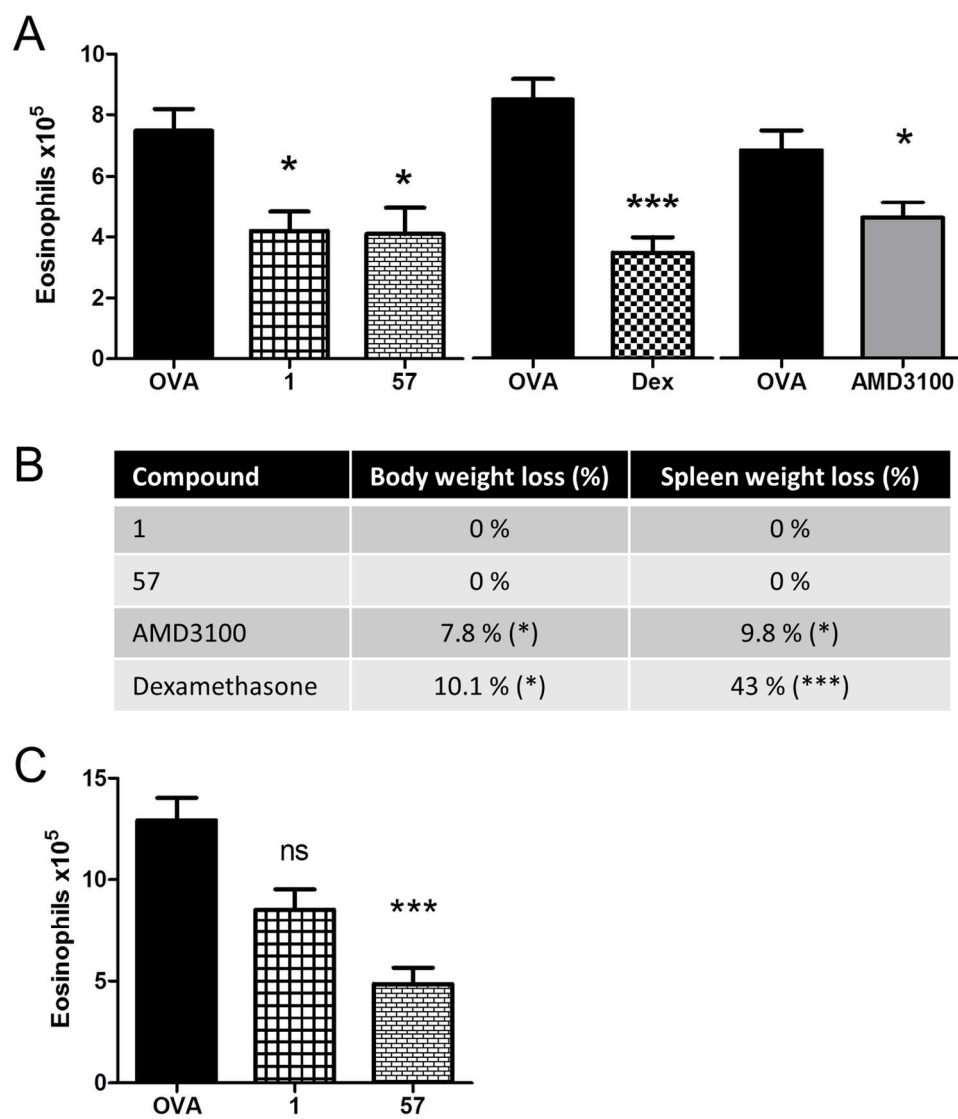


Figure 8

133x151mm (300 x 300 DPI)